Lecture Notes on the Nuclear Shell Model

Ragnar Stroberg
TRIUMF

December 11, 2015

Abstract

The nuclear shell model is a powerful tool for understanding nuclear structure. In its simplest form, it provides an intuitive picture of nuclei and a reasonably reliable way to predict nuclear properties with simple analytic calculations. In it's more elaborate incarnations, it is a computational framework which can allow for a quantitative description of experimental data, including collective phenomena which are typically not associated with the shell model. In these lectures, I will discuss some of the intuitive aspects and then outline the steps taken to move to the more quantitative modern large-scale shell model calculations.

At all points, I will attempt to stress understanding of the physics over any involved calculation. If a picture can clearly convey an idea, it is preferred over an equation. It is hoped that any interested student can then persue more technical details in one of the references provided at the end of these notes.

Contents

Chapter 1

Many-body wave functions, angular momentum, and tensor algebra

In these lectures, we will treat the nucleus as a non-relativistic, fermionic many-nucleon quantum system. Thinking about such a complicated system is inherently difficult, but can be made somewhat less painful by employing the right formalism. I'll begin by reviewing some elements of non-relativistic quantum mechanics which will be used in this course. This will serve the dual purpose of filling any gaps from your previous courses, and acquainting you with my choice of notation before moving on to new concepts.

1.1 Angular momentum of one particle

The operators $\hat{J}_x, \hat{J}_y, \hat{J}_z$ characterize the angular momentum of a particle about the x, y, z directions, respectively. They obey the commutation relation

$$[\hat{J}_i, \hat{J}_j] = i\epsilon^{ijk}\hat{J}_k \tag{1.1}$$

(where ϵ^{ijk} is the Levi-Civita symbol for an anti-symmetric tensor) and so we cannot construct a simultaneous eigenstate of more than one component of the angular momentum vector $\hat{\vec{J}}$. [1]

On the other hand, the operator $\hat{J}^2 = \hat{J}_x{}^2 + \hat{J}_y{}^2 + \hat{J}_z{}^2$ commutes with each of the $\hat{J}_i$ individually.

[1] This can be understood easily in the case of orbital angular momentum $\hat{L}_i = \hat{r}_j\hat{p}_k\epsilon^{ijk}$. If all three components were well-defined, then one could rotate the coordinates such that $\vec{L}$ coincided with the z-axis. Then this would require $L_x = L_y = 0$, and the particle would be orbiting in a plane with well-defined $p_z = r_z = 0$, which would very much upset Dr. Heisenberg. Spin angular momentum, which obeys the same commutation relation, has no classical analogue and so is trickier to think about.

We may therefore construct a simultaneous eigenstate of $\hat{J}^2$ and one component, which we take to be J_z. We indicate this state $|jm\rangle$, with eigenvalues

$$\hat{J}^2|jm\rangle = j(j+1)|jm\rangle \quad \hat{J}_z|jm\rangle = m|jm\rangle. \tag{1.2}$$

We can construct the angular momentum raising and lowering operators

$$\hat{J}_+ \equiv \hat{J}_x + i\hat{J}_y \quad , \quad \hat{J}_- \equiv \hat{J}_x - i\hat{J}_y. \tag{1.3}$$

When these operators act on a state $|jm\rangle$, they produce

$$\hat{J}_\pm|jm\rangle = \sqrt{j(j+1) - m(m\pm 1)}|jm\pm 1\rangle. \tag{1.4}$$

1.2 Angular momentum of two particles

If we have two particles in orbits which are each eigenstates of the $\hat{J}^2$ operator with quantum numbers j_1 and j_2, we may also measure the total angular momentum of the system with

$$\vec{\hat{J}} = \vec{\hat{J}}_1 + \vec{\hat{J}}_2 \tag{1.5}$$

$$\begin{aligned} \hat{J}^2 &= (\vec{\hat{J}}_1 + \vec{\hat{J}}_2)\cdot(\vec{\hat{J}}_1 + \vec{\hat{J}}_2) \\ &= \hat{J}_1^2 + \hat{J}_2^2 + 2\vec{\hat{J}}_1\cdot\vec{\hat{J}}_2 \end{aligned} \tag{1.6}$$

We can see that $[\hat{J}_{1z}, \hat{J}^2] \neq 0$, so we cannot construct a simultaneous eigenstate of $\hat{J}^2$ and $\hat{J}_{1z}$. If we construct a state with good total angular momentum J, then m_1 and m_2 are no longer good quantum numbers. However, $\hat{J}_z = \hat{J}_{1z} + \hat{J}_{2z}$ does commute with $\hat{J}$, and so we can construct an eigenstate of $\hat{J}^2$ and $\hat{J}_z$ with eigenvalues $J(J+2)$ and M, respectively.

$$|j_1 j_2 JM\rangle = \sum_{m_1 m_2} \langle j_1 m_1 j_2 m_2 | j_1 j_2 JM\rangle |j_1 m_1 j_2 m_2\rangle. \tag{1.7}$$

The overlap $\langle j_1 m_1 j_2 m_2 | j_1 j_2 JM\rangle$ is called a Clebsch-Gordan coefficient.

1.3 Angular momentum of three particles

If we get a little more fancy, we can consider three particles with angular momenta j_1, j_2, j_3 coupled to total angular momentum J. We just couple j_1 and j_2 to J_{12}, and then couple j_3 and J_{12} to J, and we have

$$|(j_1 j_2 J_{12}) j_3 JM\rangle = \sum_{m_1 m_2 J_{12}} \langle j_1 m_1 j_2 m_2 | J_{12} M_{12}\rangle \langle J_{12} M_{12} j_3 m_3 | JM\rangle |j_1 m_2 j_2 m_2 j_3 m_3\rangle. \tag{1.8}$$

Note that we could have instead coupled j_2 and j_3 to J_{23} and then coupled j_1 and J_{23} to J. The conversion between these two coupling schemes is given by

$$\begin{aligned}&\langle (j_1 j_2 J_{12}) j_3 m_3 JM | j_1 (j_2 j_3 J_{23}) JM \rangle \\ &\qquad = (-1)^{j_1+j_2+j_3+J} \sqrt{2J_{12}+1}\sqrt{2J_{23}+1} \begin{Bmatrix} j_1 & j_2 & J_{12} \\ j_3 & J & J_{23} \end{Bmatrix}\end{aligned} \tag{1.9}$$

The symbol in curly brackets is called a $6j$ symbol, and may be computed by several methods which are relatively unenlightening for the physics we want to study.

1.4 Quantum numbers

The quantum numbers of a state are conserved if their corresponding operator commutes with the Hamiltonian. In general, we will consider rotationally invariant Hamiltonians, which means that total angular momentum J will be conserved. Depending on our choice of single-particle basis, we can have various other quantum numbers as well, such as the number of radial nodes n, spin and orbital angular momentum s and ℓ, their projections m_s,m_ℓ, etc. In addition to radial and angular momentum quantum numbers, we have parity and – if we choose – isospin.

1.4.1 Parity

The parity operator $\mathcal{P}$ reflects the three spatial directions $\vec{r} \to -\vec{r}$. If $\mathcal{P}$ commutes with the Hamiltonian (which it does, approximately), then eigenstates of the Hamiltonian can be eigenstates of $\mathcal{P}$ with eigenvalue π

$$\mathcal{P}|\Psi\rangle = \pi|\Psi\rangle \tag{1.10}$$

Applying $\mathcal{P}$ twice takes us back to where we started, so $\pi^2 = 1$ and $\pi = \pm 1$. For a single-particle orbit the parity is given by $\pi = (-1)^\ell$, with ℓ the orbital angular momentum. This follows from the parity of the spherical harmonics.

1.4.2 Isospin

Empirically, the masses of the proton and neutron are very close, and the proton-proton and neutron-neutron interactions are very nearly the same (aside from the Coulomb interaction), and so it is a reasonable approximation to treat them as the same type of particle (the nucleon) with an additional property called isospin, denoted t. The mathematics of isospin is identical to that of spin-$\frac{1}{2}$. The two possible projections, $t_z = +\frac{1}{2}$ and $t_z = -\frac{1}{2}$ correspond to a neutron and a proton, respectively. (This is the nuclear physics convention, chosen so that most nuclei have positive isospin. The convention in particle physics is the opposite.) If we work in the isospin formalism, then the orbits are labeled by n,ℓ,j,m_j,t_z [2].

[2] Total isospin t is omitted for the same reason as s.

Two nucleons can couple to total isospin $T = 0$ or $T = 1$, with corresponding projections T_z. Three nucleons can couple to total isospin $\frac{1}{2}$ or $\frac{3}{2}$, and so on. Isospin can be a difficult concept to grasp. The physical meaning of the isospin projection is clear: it's simply given by $T_z = \frac{N-Z}{2}$. However, the meaning of the magnitude is less clear. If two nucleons have $T_z = 0$, meaning one is a proton and one is a neutron, this can be achieved with either $T = 0$ or $T = 1$. So what's the difference? How can we tell what the total isospin should be?

The difference is symmetry. Just as is done with spins, two isospins can be combined into symmetric and antisymmetric combinations. The symmetric combination

$$|\mathcal{S}\rangle = \frac{1}{\sqrt{2}}(|\uparrow\rangle + |\downarrow\rangle) \tag{1.11}$$

has $T = 1$, while the antisymmetric combination

$$|\mathcal{A}\rangle = \frac{1}{\sqrt{2}}(|\uparrow\rangle - |\downarrow\rangle) \tag{1.12}$$

has $T = 0$. Nucleons are fermions, and so the total many-nucleon wave function must be antisymmetric. For two-nucleon system, consider the case where $L = 0$ and $S = 1$, i.e. the spatial and spin components of the wave function are symmetric. This means that we must have $T = 0$ in order to have overall antisymmetry. On the other hand, if we have $L = 0$ and $S = 0$ (spin antisymmetric), then we need $T = 1$. Note that for a neutron-neutron system with $T_z = 1$, we are restricted to $T = 1$, and so the spin-spatial part of the wave function must be antisymmetric, just as we would expect for identical particles.

There remains the question of whether or not isospin is a good quantum number for nuclei. This is again equivalent to asking whether $[H, T] = 0$ and $[H, T_z] = 0$. The latter is simpler to answer. The strong and electromagnetic interactions do not change protons into neutrons, or vice versa. The existence of beta decay tells us that T_z is not perfectly conserved, but it is conserved to a very good approximation, and so it is useful to consider T_z to be a good quantum number.

For the magnitude T, we can consider that to a first approximation the Coulomb interaction will just be proportional to $Z^2 \sim (A - T_z)^2$, which commutes with T. However, upon more detailed inspection, the Coulomb potential is not uniform, but instead has some r dependence. As a result, a proton wave function will not be exactly the same as a neutron wave function, given the same mean field. If we begin with an energy eigenstate and assign it an isospin T and projection $T_z = T$ and perform an isospin rotation to $T_z = T-1$, we will end up with a state that is not an eigenstate of the Hamiltonian. The true eigenstate will then have a mixture of different T, and so T is not a good quantum number.

1.5 Many-body wave function, Slater determinants

Here and throughout these notes, I will use $|a\rangle$ to indicate a single-particle state $|\phi_a\rangle$ in the chosen basis. The label a stands for all the quantum numbers required to specify a given state. The state $|ab\rangle$ indicates a product of single-particle states $|\phi_a\rangle|\phi_b\rangle$.

When we consider a many-body system of fermions, we need to ensure that the entire wave function is antisymmetric under particle exchange. For a two-particle system, this is achieved by

$$|ab\rangle^{\mathcal{A}} = \frac{1}{\sqrt{2}}(|ab\rangle - |ba\rangle) \tag{1.13}$$

We can see that

$$|ab\rangle^{\mathcal{A}} = -|ba\rangle^{\mathcal{A}} \tag{1.14}$$

In general, an antisymmetric A-body state can be written as a determinant

$$|ab\ldots\rangle^{\mathcal{A}} = \frac{1}{\sqrt{A!}}\begin{vmatrix} a_1 & a_2 & \ldots & a_A \\ b_1 & b_2 & \ldots & b_A \\ \vdots & \vdots & \ddots & \vdots \end{vmatrix} \tag{1.15}$$

For example, an antisymmetric three-body state is

$$|abc\rangle^{\mathcal{A}} = \frac{1}{\sqrt{6}}\begin{vmatrix} a_1 & a_2 & a_3 \\ b_1 & b_2 & b_3 \\ c_1 & c_2 & c_3 \end{vmatrix} = \frac{1}{\sqrt{6}}\big(|abc\rangle + |bca\rangle + |cab\rangle - |cba\rangle - |acb\rangle - |bac\rangle\big) \tag{1.16}$$

and we can see that

$$\begin{aligned} |abc\rangle^{\mathcal{A}} &= -|bac\rangle^{\mathcal{A}} = -|cba\rangle^{\mathcal{A}} = -|acb\rangle^{\mathcal{A}} \\ &= +|bca\rangle^{\mathcal{A}} = +|cab\rangle^{\mathcal{A}} \end{aligned} . \tag{1.17}$$

From now on, we will assume that the $\mathcal{A}$ is implied and all many-body states are antisymmetrized.

1.6 Second-quantized operator notation

The antisymmetrization of the many-body state can be more conveniently expressed using the language of second quantization. We define a vacuum state $|0\rangle$, which represents a state with no particles. We also define a creation operator $a_a^\dagger$, which creates a particle in state a

$$\begin{aligned} |a\rangle &= a_a^\dagger|0\rangle \\ |ab\rangle &= a_a^\dagger a_b^\dagger|0\rangle \end{aligned} \tag{1.18}$$

and the corresponding annihilation operator

$$a_a|a\rangle = |0\rangle. \tag{1.19}$$

We may also define the bra state

$$\langle a| = \langle 0|a_a \tag{1.20}$$

The fermi statistics of the many-body state are encoded in the $a^\dagger$ operators:

$$|ab\rangle = -|ba\rangle \quad \Rightarrow \quad a_a^\dagger a_b^\dagger = -a_b^\dagger a_a^\dagger \tag{1.21}$$

This may be written in terms of an *anticommutation relation*:

$$\{a_a^\dagger, a_b^\dagger\} \equiv a_a^\dagger a_b^\dagger + a_b^\dagger a_a^\dagger = 0. \tag{1.22}$$

In particular, we can see that the state

$$a_a^\dagger|a\rangle = |aa\rangle = a_a^\dagger a_a^\dagger|0\rangle = \frac{1}{2}\{a_a^\dagger, a_a^\dagger\}|0\rangle = 0 \tag{1.23}$$

cannot exist, in accordance with the Pauli principle.

It should be noted that, while these operators are mathematically similar to the raising and lowering operators typically encountered in discussions of the harmonic oscillator, they are physically distinct. [3] The creation operators discussed here are more closely related to the creation operators of field theory, which create a particle in a particular state. At the energy scales considered here, we don't need to consider actual nucleons being created and annihilated. However, the second-quantized formalism still provides a convenient way to treat the Fermi statistics of the system. Throughout this course, we will assume an anti-symmetrized many-body wave function unless otherwise noted.

1.7 Spherical tensors

Formally, a spherical tensor operator T_μ^λ of rank λ is a set of $2\lambda + 1$ operators ($\mu = -\lambda \ldots \lambda$) which obey the commutation relations with the J operators

$$\begin{aligned} [J_\pm, T_\mu^\lambda] &= \sqrt{\lambda(\lambda+1) - \mu(\mu \pm 1)}\, T_{\mu\pm1}^\lambda \\ [J_z, T_\mu^\lambda] &= \mu T_\mu^\lambda. \end{aligned} \tag{1.24}$$

What does this mean physically? It means that the operator T_μ^λ behaves like something that has angular momentum λ and projection μ. In the case of an electric dipole transition (we will discuss this later), the operator is rank 1 and describes the creation of an electric dipole photon, which carries angular

[3] The possibility of confusion is exacerbated by the fact that we often employ a harmonic oscillator single-particle basis.

momentum $\lambda = 1$. In fact, using the second-quantized notation, the state $|jm\rangle$ can be written as a creation operator $a^\dagger_{jm}$ acting on the vacuum

$$|jm\rangle = a^\dagger_{jm}|0\rangle \tag{1.25}$$

and $a^\dagger_{jm}$ is a spherical tensor operator. In all the cases we consider in these lectures, spherical tensor operators correspond to the adding or removing of some object with angular momentum. As a specific example, let us consider the spin operator $\vec{s} = (s_x, s_y, s_z)$ in Cartesian coordinates. In this representation, $\vec{s}$ is a rank-1 Cartesian tensor, also known as a vector. To rewrite this as a spherical tensor, we define

$$\begin{aligned} s^1_{\pm 1} &= \mp \frac{1}{\sqrt{2}}(s_x \pm i s_y) \\ s^1_0 &= s_z. \end{aligned} \tag{1.26}$$

We can check, for example, using $J_+ = J_x + iJ_y$,

$$\begin{aligned} \left[J_+, s^1_0\right] &= \left[s_+, s^1_0\right] \\ &= [s_x, s_z] + i\,[s_y, s_z] \\ &= -is_y - s_x \\ &= \sqrt{2}s^1_{+1}. \end{aligned} \tag{1.27}$$

Note in this case that while $\vec{s}$ acts on a spin-$\frac{1}{2}$ particle, it is a rank-1 tensor. This is because flipping the spin of a spin-$\frac{1}{2}$ particle requires a change $\Delta J = 1$. In a Gamow-Teller decay, whose operator is proportional to $\vec{s}$, the electron and antineutrino are emitted in an $S = 1$ state, so the rank of the operator reflects the angular momentum carried away. Since total angular momentum is conserved, the s_+ component of the nuclear operator corresonds to $S_z = -1$ for the leptons.

1.8 The Wigner-Eckart theorem

One very nice property of the matrix elements of spherical tensor operators is the fact that they may be factorized into a piece which depends on the details of the operator, and one which depends on the angular momentum coupling. The Wigner-Eckart theorem is essentially an existence theorem that this factorization exists. For some spherical tensor operator T^λ_μ, the matrix element between two state with total angular momentum J and J' is given by [4]

$$\left\langle \alpha J M \middle| T^\lambda_\mu \middle| \alpha' J' M' \right\rangle = \left\langle \alpha J \middle\| T^\lambda \middle\| \alpha' J' \right\rangle \frac{\langle J' M' \lambda \mu | J M \rangle}{\sqrt{2J+1}} \tag{1.28}$$

[4] There is some freedom in how one defines the reduced matrix element, in terms of phase factors and factors of $2J + 1$, etc. Here I follow the convention of Edmonds, which is perhaps the most common, but far from universal.

This is convenient in practical calculations because we must now only store and deal with one matrix element, rather than $2\lambda + 1$ matrix elements. In addition, in many cases such as in gamma decay, we end up summing over initial and final projections, and the result becomes a sum over Clebsch-Gordan coefficients multiplied by the reduced matrix element.

As an example, we can calculate the reduced matrix element of the spin operator for a spin $\frac{1}{2}$ state.

$$\begin{aligned} \langle\uparrow|s_0|\uparrow\rangle &= \left\langle \frac{1}{2} \middle\| s^1 \middle\| \frac{1}{2} \right\rangle \frac{\left\langle \frac{1}{2}\frac{1}{2}10 \middle| \frac{1}{2}\frac{1}{2} \right\rangle}{\sqrt{2\cdot\frac{1}{2}+1}} \\ \frac{1}{2} &= \left\langle \frac{1}{2} \middle\| s^1 \middle\| \frac{1}{2} \right\rangle \frac{1/\sqrt{3}}{\sqrt{2}} \\ \left\langle \frac{1}{2} \middle\| s^1 \middle\| \frac{1}{2} \right\rangle &= \sqrt{\frac{3}{2}}. \end{aligned} \tag{1.29}$$

1.9 Exercises

1. Here we will calculate some Clebsch-Gordan coefficients. In the fully-stretched case, the coefficient is 1, i.e. $\langle j_1 m_1, j_2 m_2 | j_1 j_2 J M\rangle = 1$ for $m_1 = j_1$, $m_2 = j_2$, and $J = M = j_1 + j_2$. By applying the lowering operator J_- to $\langle j_1 m_1 j_2 m_2|$ and $|j_1 j_2 J M\rangle$, calculate the Clebsch-Gordan coefficent $\langle 1010|1120\rangle$.

2. Show that the other equations in (1.24) are also satisfied for the operator $\vec{s}$.

3. How should the two-particle bra state $\langle ab|$ be written in second-quatized notation, in order to maintain normalization $\langle ab|ab\rangle = 1$?

Chapter 2

Nuclear forces

2.1 Origin of the force between nucleons

Protons and neutrons interact primarily via the strong nuclear force, which is an effect of quantum chromodynamics (QCD), but is distinct from the force between two quarks.

We can think of the nuclear force in analogy to the van der Waals force between neutral, non-polar atoms. At large distances, there is no Coulomb force between two neutral atoms. However, as the atoms are moved closer together, the electrons in one atom become correlated with the electrons in the other, reducing the total energy. This is often described as an instantantaneous dipole moment in one atom inducing a dipole moment in the other, with a resulting attractive dipole-dipole interaction. Similar effects can occur in higher multipoles.

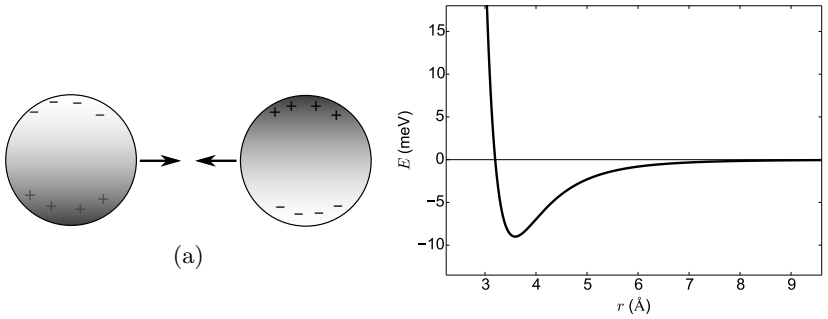

(a)

(b)

Figure 2.1: (a) The van der Waals attraction between two neutral atoms. (b) The Lennard-Jones potential which parameterizes the attractive polarization and repulsive exchange effects.

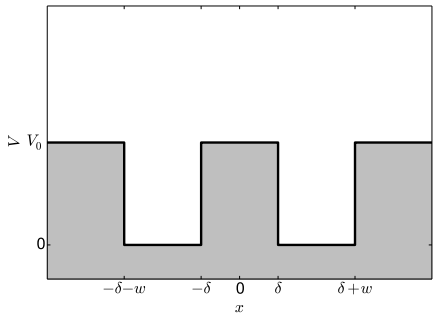

Figure 2.2: The finite well potential

Another effect becomes important at short distances – namely the fact that the electrons in the atom are fermions – leading to an effect which is often called Pauli blocking, or the exchange interaction. As a simplified illustration of how the exchange interaction works, consider two particles in a one-dimensional finite square well potential [1].

$$V(x) = \begin{cases} 0 & \delta < |x| < \delta + w \\ V_0 & \text{otherwise} \end{cases} \tag{2.1}$$

The eigenvalues can't be obtained analytically for this system, but they can be found numerically quite easily. Figure 2.3(a) shows the wave functions for two different separations, while (b) shows the energy as a function of δ. The important point is that when we have two particles in two wells, we cannot simply treat them as distinct particles in their original eigenstates. Both particles see both potential wells, and so one particle will occupy the global ground state, and the second will occupy the first excited state. At large δ, the ground state and first excited states are essentially degenerate and the total energy is independent of δ; the two different wells can be considered as separate. However, at short distances, the degeneracy breaks and the total energy increases sharply. In the limit $\delta \to 0$, we simply have a finite well potential of width $2w$. This increase in energy is essentially the effect of the Pauli principle, and leads to a hard-core repulsion at short distances.

A totally analogous effect occurs in the interaction between nucleons, with the electrons replaced by quarks, and the electromagnetic interaction replaced by the strong interaction. Another important feature of this type of interaction between composite particles is that the presence of a third particle will polarize the other two, and change the way they interact. This effect manifests itself as an *irreducible* three-body force (irreducible meaning that some part of the interaction between three nucleons cannot be expressed as the linear sum

[1] see, e.g., Ch.11 of [3], `http://www.physics.utah.edu/~lebohec/P5450/Posting/exact_double_well_schrodinger.pdf`, and `http://www.hep.manchester.ac.uk/u/forshaw/BoseFermi/Double%20Well.html`

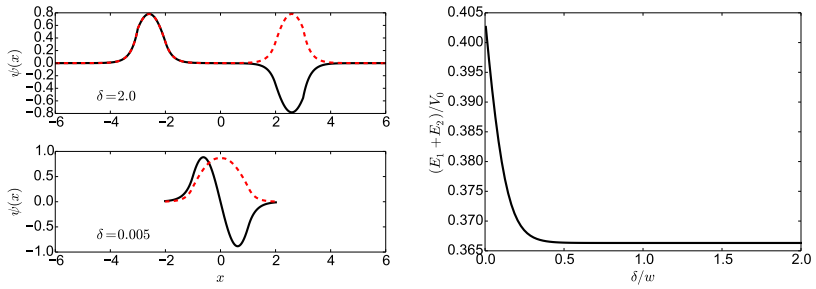

(a) (b)

Figure 2.3: (a) Wave functions of the two lowest eigenstates for the semi-finite well potential with two different δ, for $w = 1, V_0 = 10$. (b) Total energy as a function of the separation δ.

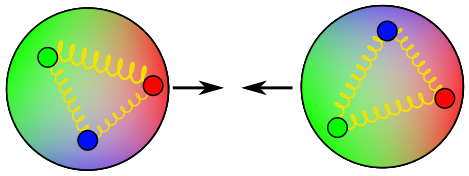

Figure 2.4: The force between nucleons caused by instantaneous polarization of the color charge distribution.

of pairwise interactions). We therefore expect that many-body forces will be present, although at this point we cannot estimate their magnitude relative to two-body forces.

2.2 The one pion exchange potential

The van der Waals potential betwen atoms may be expanded in terms of induced multipole moments, with the dipole moment being the longest range at r^{-3}. In a similar way, the more complicated nuclear force can be expanded in terms of hadronic fields. At "long" distances ($\gtrsim$1.5 fm) the interaction between nucleons can be modeled as an exchange of pions. The potential due to a static pion field, in analogy to a static Coulomb field, is given by

$$\begin{aligned} V_\pi(r) &= -\frac{f_\pi^2}{4\pi m_\pi}(\tau_1\cdot\tau_2)(\sigma_1\cdot\nabla_1)(\sigma_2\cdot\nabla_2)\frac{e^{-m_\pi r}}{r} \\ &= \frac{f_{\pi^2}}{12\pi}\tau_1\cdot\tau_2\left[\sigma_1\cdot\sigma_2\left(\frac{e^{-m_\pi r}}{r}-\frac{4\pi}{m_\pi^2}\delta(r)\right)+\mathbf{S}_{12}(r)\left(1+\frac{3}{m_\pi r}+\frac{3}{m_\pi^2 r^2}\right)\frac{e^{-m_\pi r}}{r}\right] \end{aligned} \tag{2.2}$$

where the $\frac{e^{-m_\pi r}}{r}$ Yukawa term reflects the fact that the pion has a non-zero mass and therefore finite range, the $(\tau_1\cdot\tau_2)$ term reflects that the pion is isovector

($T = 1$, with the three projections corresponding to π^+, π^0, π^-), and the $(\sigma_1 \cdot \nabla_1)$ terms reflect that the pion is a pseudoscalar ($J^\pi = 0^-$). A more detailed derivation is beyond the scope of these lectures, but may be found in [1], among other places.

The quantity $\tau_1 \cdot \tau_2$ (and likewise $\sigma_1 \cdot \sigma_2$) can be evaluated by noting

$$\begin{aligned} T^2 &= t_1^2 + t_2^2 + 2t_1 \cdot t_2 \\ \tau_1 \cdot \tau_2 &= 2T(T+1) - 3 \end{aligned} \tag{2.3}$$

So $\tau_1 \cdot \tau_2 = -3$ for $T = 0$ and 1 for $T = 1$. Thus we can see that pion exchange is of opposite sign for pp, nn and for pn and the strength is twice as much for pn.

2.3 Central, spin-orbit, and tensor components

One way to classify the components of the two-body nuclear force is in terms of the tensor rank of the spins. Two spins may be combined to form a rank 0, 1, or 2 tensor. The rank-0, or scalar, components are either independent of the spins, or have a $\sigma_1 \cdot \sigma_2$ dependence. This is the most familiar form of potential, since it depends on the magnitude of the vector $|\vec{r}|$ between the two nucleons.

The rank-1, or vector, components – sometimes referred to as the spin-orbit components – involve $\vec{S} = \vec{\sigma_1} + \vec{\sigma}_2$. Since the energy is a scalar, this needs to be combined with another vector, such as the relative orbital angular momentum $\vec{L}$, to form a scalar like $\vec{L} \cdot \vec{S}$. This turns out to be a relatively minor component of the nuclear interaction. One should keep in mind that the $\vec{L}$ used here is the relative orbital angular momentum of the two-nucleon subsystem, and so it is not directly related to the one-body spin-orbit splitting of the simple shell model we will discuss later.

The rank-2 components, generally referred to as the tensor components, involve the spins coupled to a rank-2 tensor.

$$[\sigma_1 \otimes \sigma_2]^{(2)}_\mu = \sum_{\mu_1 \mu_2} \langle 1\mu_1 1\mu_2 | 2\mu \rangle \sigma_{1\mu_1} \sigma_{2\mu_2} \tag{2.4}$$

This rank-2 tensor is then coupled with another rank-2 tensor, such as $Y^{(2)}(\hat{r})$ to form a scalar.

$$\begin{aligned} \mathbf{S}_{12} &= [\sigma_1 \otimes \sigma_2]^{(2)} \cdot Y^{(2)}(\hat{r}) \\ &= (\vec{\sigma}_1 \cdot \hat{r})(\vec{\sigma}_2 \cdot \hat{r}) - \frac{1}{3} \vec{\sigma}_1 \cdot \vec{\sigma}_2 \end{aligned} \tag{2.5}$$

This component is the most difficult to visualize, because it depends on the relative positions of the nucleons and the orientations of their spins in a non-trivial way. One way to understand the tensor force is to consider values of $\mathbf{S}_{12}$ for various classical configurations. In fact, this type of interaction is not totally unfamiliar; the interaction between two bar magnets is of precisely this form.

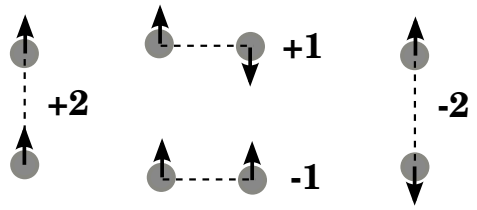

Figure 2.5: Values of $3 \times \mathbf{S}_{12}$ for various configurations of two particles with spin.

2.4 The deuteron

The deuteron is the only bound two-nucleon system, and it can give us some insight into the nuclear force. It is bound by just 2.2 MeV, with ground state spin and parity $J^\pi = 1^+$, while the two-proton and two-neutron systems are unbound.

In order to form a 1^+ state, the nucleons must be in an $S = 1$ state with $L = 0$ or $L = 2$, and we would assume that the $L = 0$ state would be the ground state. However, the quadrupole moment of the deuteron is measured to be 28.6 fm^2, which is impossible for a pure $L = 0$ state. This means that the deuteron ground state contains at least some $L = 2$ component (the asymptotic D/S ratio is listed as about 2.5%). The fact that $L = 0$ and $L = 2$ are mixed by the nuclear interaction led to the proposal of a tensor component of the nuclear force, which we have seen arises from a one-pion exchange potential.

Furthermore, since we have $S = 1$ and even L, which are both symmetric under particle exchange, the deuteron must be $T = 0$. Since the pp and nn systems are unbound, and there is no bound $T = 1$ state in the deuteron, we can surmise that the nucleon-nucleon interaction is more attractive in the $T = 0$ channel. Another interpretation would be that the nuclear force is more attractive for aligned spins.

2.5 Exercises

1. Explain, from a proton-neutron point of view, why $T = 0$ is antisymmetric and $T = 1$ is symmetric.

2. Explain the same thing from an isospin point of view.

3. Why can't the deuteron ground state have an $L = 1$ component?

4. Can you think of any possible sources of isospin symmetry breaking in the nuclear interaction?

Chapter 3

Shell structure and single-particle motion

3.1 Evidence/Motivation

The evidence of shell structure in nuclei may be seen by considering the systematics of nuclear binding energies relative to the predictions of the liquid drop model (LDM). The LDM accounts for bulk attraction, surface effects, Coulomb effects, symmetry energy, and pairing. Clearly, there is some other effect which makes nuclei with neutron numbers N=2, 8, 20, 28, 50, 82, and 126 particularly well-bound. The same *magic numbers* are observed for protons. It was long suspected that this was due to shell effects, analogous to what is observed in atomic structure. However, with the assumption of a independent nucleons moving in a mean-field harmonic oscillator potential – a reasonable first guess for well-bound nucleons – the shell gaps arise at nucleon numbers 2, 8, 20, 40, 70..., which is promising, although something is clearly missing. Resolution came when Maria Mayer and Hans Jensen suggested the addition of a potential term with a strong spin-orbit coupling – that is, proportional to $\vec{\ell} \cdot \vec{s}$. With this assumption, all the known magic numbers were reproduced. Further, with this model they were able to predict the ground-state spin and parity of odd-mass nuclei which could be interpreted as one nucleon above a shell gap, the systematics of magnetic moments, and the presence of "islands of isomerism".

3.2 The nucleus as a Fermi liquid

While the successes of the independent particle model present a strong case, we ought to consider how plausible it actually is. Nuclear radii are on the order of a few fm, while the radii of nucleons is slightly less than 1 fm, suggesting that, semi-classically, the spacing between nucleons is on the order of the size of the nucleons. How is it, then, that we can reasonably treat nucleons as moving in

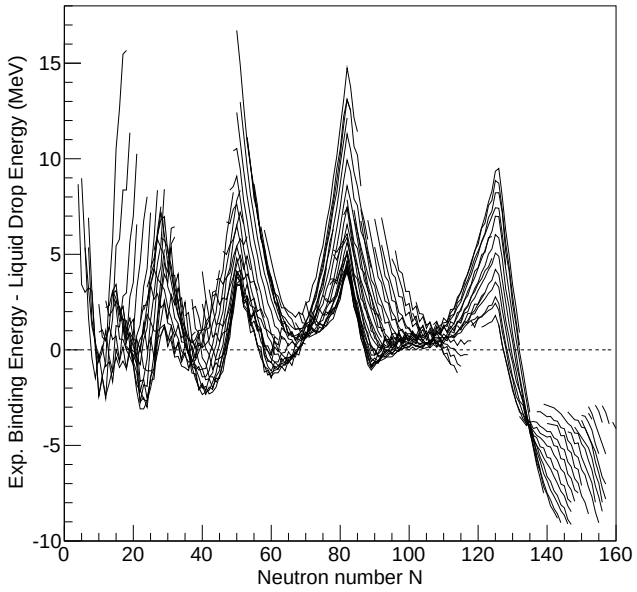

Figure 3.1: Experimental binding energies of isotopic chains, relative to the liquid drop model prediction.

uninterrupted orbits?

To address this, we consider the theory of Fermi liquids, developed by Landau to describe condensed matter systems. We begin with a non-interacting Fermi gas in some mean field potential. In the ground state all orbits are filled up to the Fermi level, above which no orbits are filled. The low-lying excitation spectrum will consist of particle-hole excitations across the Fermi surface.

$$\begin{aligned} E_{ph} &= E_0 + \epsilon_p - \epsilon_h \\ E_{pp'hh'} &= E_0 + \epsilon_p + \epsilon_{p'} - \epsilon_h - \epsilon_{h'} \end{aligned} \tag{3.1}$$

Here, ϵ_p and ϵ_h are the energies of the particle and hole states, respectively. We now imagine turning on a weak interaction δV between the particles. If we do this adiabatically, and making some other assumptions about avoiding phase transitions, then the excitation spectrum does not change discontinuously and there remains a one-to-one correspondence between the excited states of the interacting and non-interacting systems.

This suggests that we may write the energy if the interacting system as before, but with modified single-particle energies:

$$\begin{aligned} E_{ph}(\delta V) &\approx E_0(\delta V) + \epsilon_p(\delta V) - \epsilon_h(\delta V) \\ E_{pp'hh'}(\delta V) &\approx E_0(\delta V) + \epsilon_p(\delta V) + \epsilon_{p'}(\delta V) - \epsilon_h(\delta V) - \epsilon_{h'}(\delta V) \end{aligned} \tag{3.2}$$

These $\epsilon_p(\delta V)$ now refer to the energies of *quasi-particle* states, and $\epsilon_h(\delta V)$ refer

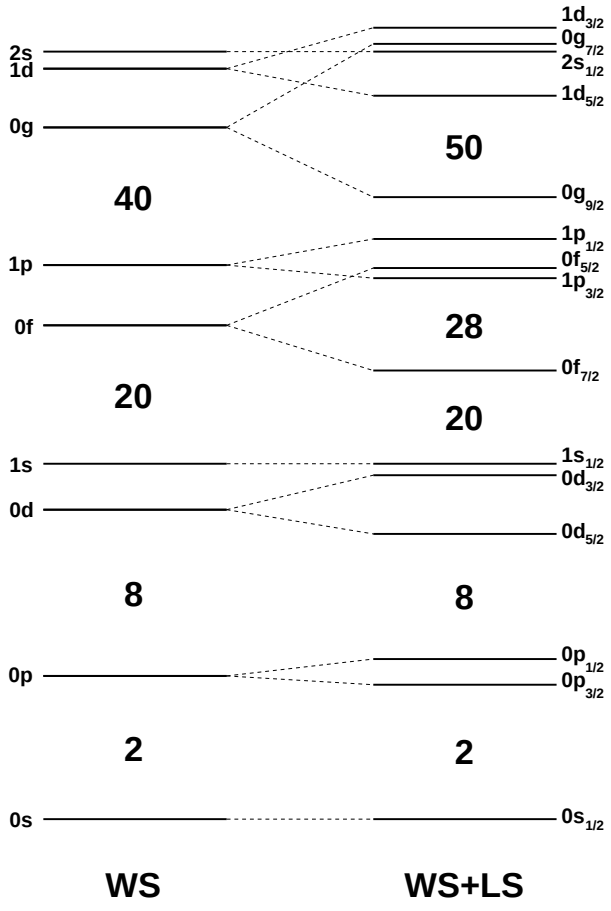

Figure 3.2: Single-particle energies for a Woods-Saxon potential (left), and a Woods-Saxon plus an attractive spin-orbit interaction (right).

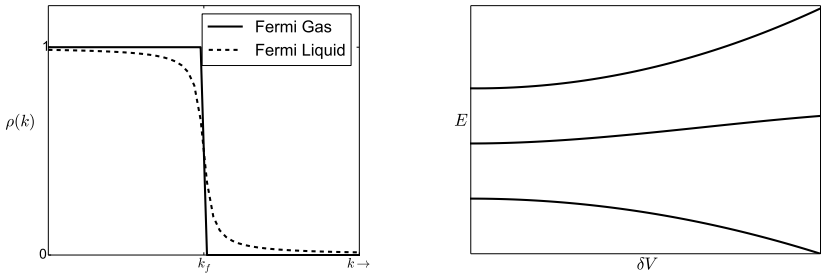

Figure 3.3: a) Schematic density of states for a Fermi gas and a Fermi liquid, with Fermi momentum k_f. b) Schematic evolution of the excitation spectrum of a Fermi liquid as a function of the interaction strength δV.

to *quasi-hole* states. Now consider the collision of two quasi-particles in the ground state of the nucleus. For the quasi-particles to collide, they require a final state which is different from the initial state, which may be described as a by quasi-particle and quasi-hole excitations. If the density of such final states is low, as it is near the Fermi surface, then the available phase space for a collision is small and collisions are rare. This at least qualitatively justifies the assumption of independent single-particle orbits.

3.3 Single-particle potentials

We now need to specify what the single-particle orbits are that we're using. This depends on the choice we make for the form of the mean-field potential.

3.3.1 Harmonic oscillator

A common choice for the potential is that of a 3D isotropic harmonic oscillator:

$$V(r) = \frac{1}{2} m\omega^2 r^2. \tag{3.3}$$

There are several appealing features of the harmonic oscillator potential which lead to its widespread use in nuclear structure calculations. First, the eigenfunctions of the harmonic oscillator potential are known analytically, and so the Schrödinger equations doesn't have to be numerically integrated to produce wave functions. Second, the wave functions for a two-particle system may be analytically factorized into relative and center-of-mass coordinates. This is important for producing a translationally-invariant Hamiltonian, because we are interested in the properties of the nucleus at rest. This is also helpful because the nucleon-nucleon interaction depends on the relative coordinate of the two nucleons, not the center-of-mass coordinate.

The greatest deficiency of the harmonic oscillator basis is that it has the incorrect asymptotic behavior. At large values of r, the short-ranged nuclear

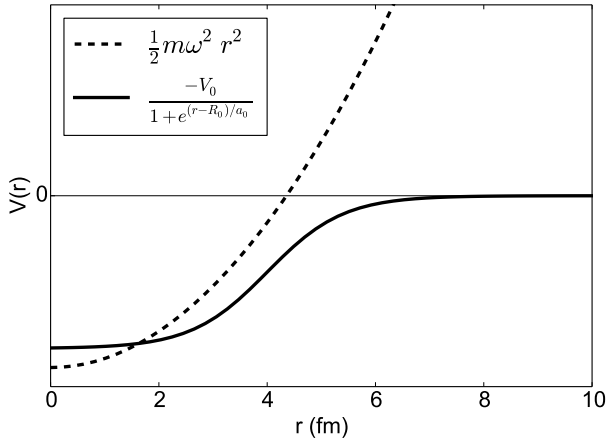

Figure 3.4: Harmonic oscillator and Woods-Saxon potentials. The oscillator potential has been shifted down in energy for comparison.

potential should go to 0. However the harmonic oscillator potential goes to infinity at large r. The result is that all eigenstates are bound states, up to infinite energy. Additionally, the wave function should die off as e^{-r/r_0}, but oscillator wave functions die off as $e^{-(r/r_0)^2}$.

3.3.2 Woods-Saxon

In order to better reflect the short-range nature of the nuclear potential, another common choice for the parameterization is the Woods-Saxon form

$$V(r) = \frac{-V_0}{1 + e^{\frac{r-R_0}{a}}}. \tag{3.4}$$

This form allows for unbound states, and yields wave functions with the proper asymptotic behavior. However, no closed-form solution exists, and so wave functions must be found numerically, making the Woods-Saxon potential more difficult to work with.

3.3.3 Hartree-Fock

Since the mean field for one nucleon is generated by all the other nucleons, a natural way to generate the potential is to obtain a self-consistent mean field by the Hartree-Fock method, assuming we have a reasonable model for the force between nucleons. Since the subject of these lectures is the shell model, not Hartree-Fock, only a brief sketch of the method is given here. The algorithm is essentially

1. Begin by choosing some ansatz for the mean field potential $U^{(0)}(\vec{r})$, typically either a harmonic oscillator or Woods-Saxon potential.
2. Find the eigenfunctions $\phi_i^{(0)}(\vec{r})$ for a single particle moving in that potential.
3. Fill the A lowest-energy orbits, according to the Pauli principle.
4. Generate a new potential $U^{(1)}(\vec{r})$ by summing over the potential due to the nucleons in the filled orbits.
$$U^{(1)}(\vec{r}) = \sum_i \int d^3r' V(\vec{r} - \vec{r'}) |\phi_i^{(0)}(\vec{r'})|^2 \tag{3.5}$$
5. Find the new eigenfunctions $\phi_i^{(1)}(\vec{r}$ of the potential $U^{(1)}(\vec{r})$.
6. Iterate the procedure until $U^{(n)}(\vec{r}) = U^{(n-1)}(\vec{r})$, within some tolerance.

In the end, we have an orthogonal basis of single-particle states, which should reasonably approximate the fully-correlated wave function. This method may be carried out in one of two ways; we may numerically integrate the Schrödinger equation in coordinate space, or we may expand the Schrödinger equation on some basis (like the harmonic oscillator basis), yielding an iterative eigenvalue problem. If we choose the former approach, then the same drawback applies as did for the Woods-Saxon potential, namely that we do not have an analytic form for the wave function.

3.4 Good quantum numbers for a spin-orbit potential

As was discussed previously, a quantum number is conserved if its corresponding operator commutes with the Hamiltonian. A single particle bound by a spherically symmetric potential $V(r)$ will have a number of conserved quantum numbers: total angular momentum j and projection m_j, orbital angular momentum ℓ and projection m_ℓ, spin angular momentum s and projection m_s, and the radial quantum number n (indicating the number of nodes in the radial wave function).

In the presence of a spin-orbit potential proportional to $\vec{\ell} \cdot \vec{s}$, the projections m_ℓ and m_s are no longer good quantum numbers. This may be seen by considering the commutator

$$\begin{aligned} \left[(\vec{\ell} \cdot \vec{s}), \ell_z\right] &= [\ell_x, \ell_z]\, s_x + [\ell_y, \ell_z]\, s_y \\ &= -i\ell_y s_x + i\ell_x s_y \neq 0 \end{aligned} \tag{3.6}$$

with a similar relation holding for s_z. However, m_j is still good, which we can see by recognizing $j^2 = (\vec{\ell} + \vec{s})^2 = \ell^2 + s^2 + 2\vec{\ell} \cdot \vec{s}$, and evaluating the commutator

$$\left[(\vec{\ell} \cdot \vec{s}), j_z\right] = \frac{1}{2}\left[(j^2 - \ell^2 - s^2), j_z\right] = 0. \tag{3.7}$$

Additionally, ℓ and s are still good quantum numbers:

$$\begin{aligned}\left[(\vec{\ell}\cdot\vec{s}),\ell^2\right] &= \left[\ell_x,\ell^2\right]s_x + \left[\ell_y,\ell^2\right]s_y + \left[\ell_z,\ell^2\right]s_z = 0\\ \left[(\vec{\ell}\cdot\vec{s}),s^2\right] &= \left[s_x,s^2\right]\ell_x + \left[s_y,s^2\right]\ell_y + \left[s_z,s^2\right]\ell_z = 0\end{aligned} \tag{3.8}$$

It is therefore useful to work with orbits of good n,ℓ,s,j, and m_j. Since we are dealing with nucleons, $s = \frac{1}{2}$ always and we generally omit it.

3.5 Independent particle model (IPM)

As shown by Mayer, the assumption of independent particle motion allows the prediction of a large number of nuclear properties, particularly ground-state and excited-state spins. In the IPM, we assume that

1. A strong spin-orbit splitting lowers the energy of the $j = \ell + s$ spin-orbit partner.
2. Nucleons are placed into orbits in accordance with the Pauli principle.
3. Even numbers of identical nucleons couple to $J = 0$, and an odd number of nucleons in an orbit j couple to $J = j$.

3.5.1 Ground state spins

Within this model we can first consider ^{17}O and ^{17}F, which may be considered as one neutron and one proton outside of ^{16}O. From the levels in Figure 3.2, we can see that the relevant orbits will be $0d_{5/2}$, $0d_{3/2}$ and $1s_{1/2}$. We expect from the spin-orbit splitting that $0d_{5/2}$ will have the lowest energy, so we predict that the ground states of ^{17}O and ^{17}F will be $5/2^+$, with low-lying $1/2^+$ and $3/2^+$ excited states. This is in fact what is seen experimentally, as shown in Figure 3.5.

3.5.2 Magnetic moments

The magnetic moment of a nucleus is the vector sum of the magnetic moments of each of its constituent nucleons. The moment for a single nucleon has spin and orbital contributions. The operator is

$$\mathcal{O}(M1) = \mu_N \sum_i g_\ell \ell_z^i + g_s s_z^i. \tag{3.9}$$

where g_ℓ is the orbital g-factor, which is 1.0 for protons and 0 for neutrons, and g_s is the spin g-factor which is 5.586 for protons and -3.826 for neutrons. These values are given in units of nuclear magnetons $\mu_N = \frac{e\hbar}{2m_pc} = 1.05\ e$ fm. In the independent particle model, all of the paired nucleons will cancel out, and the magnetic moment of the entire nucleus will be zero for an even-even nucleus, or given by that of the unpaired nucleon for an odd mass nucleus.

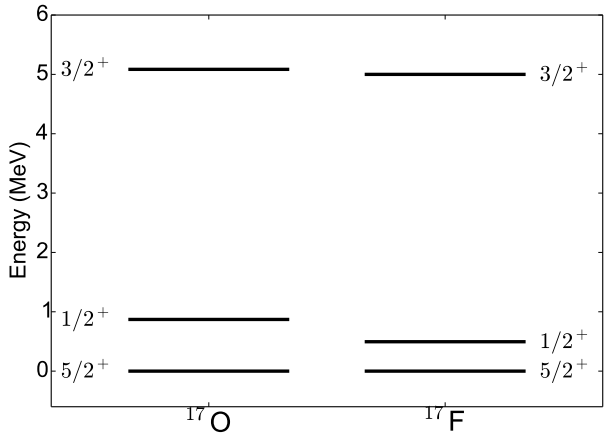

Figure 3.5: The lowest-lying even-parity states in ^{17}O and ^{17}F.

Since we measure along the projection of the total angular momentum, we have only the two possibilities $j_z = j = \ell \pm \frac{1}{2}$. For the case $j = \ell + \frac{1}{2}$, we have $\ell_z = j - \frac{1}{2}$ and $s_z = \frac{1}{2}$, resulting in

$$\mu = (j - \frac{1}{2})g_\ell + \frac{1}{2}g_s. \tag{3.10}$$

The case $j = \ell - \frac{1}{2}$ is slightly trickier. The projection s_z along the direction of j may be rewritten as

$$\begin{aligned} s_z &= (\vec{j} \cdot \vec{s})j_z/j^2 \\ &= (\vec{\ell} \cdot \vec{s} + \vec{s} \cdot \vec{s})j_z/j^2 \\ &= (\frac{j^2 - \ell^2 - s^2}{2} + s^2)j_z/j^2 \\ \langle s_z \rangle &= \frac{(j(j+1) - \ell(\ell+1) + \frac{3}{4})j}{2j(j+1)} \\ &= -\frac{j}{2(j+1)}. \end{aligned} \tag{3.11}$$

And so for $j = \ell - \frac{1}{2}$, we have

$$\mu = \frac{j(j+\frac{1}{2})}{j+1}g_\ell - \frac{j}{2(j+1)}g_s. \tag{3.12}$$

These two prections give what are called Schmidt lines, and they reproduce the observed trend in magnetic moments, although they over-predict the magnitude. Better agreement with experiment can be achieved by using a value of g_s "quenched" by a factor of ~ 0.6. This quenching provides a hint that the IPM is not the full story.

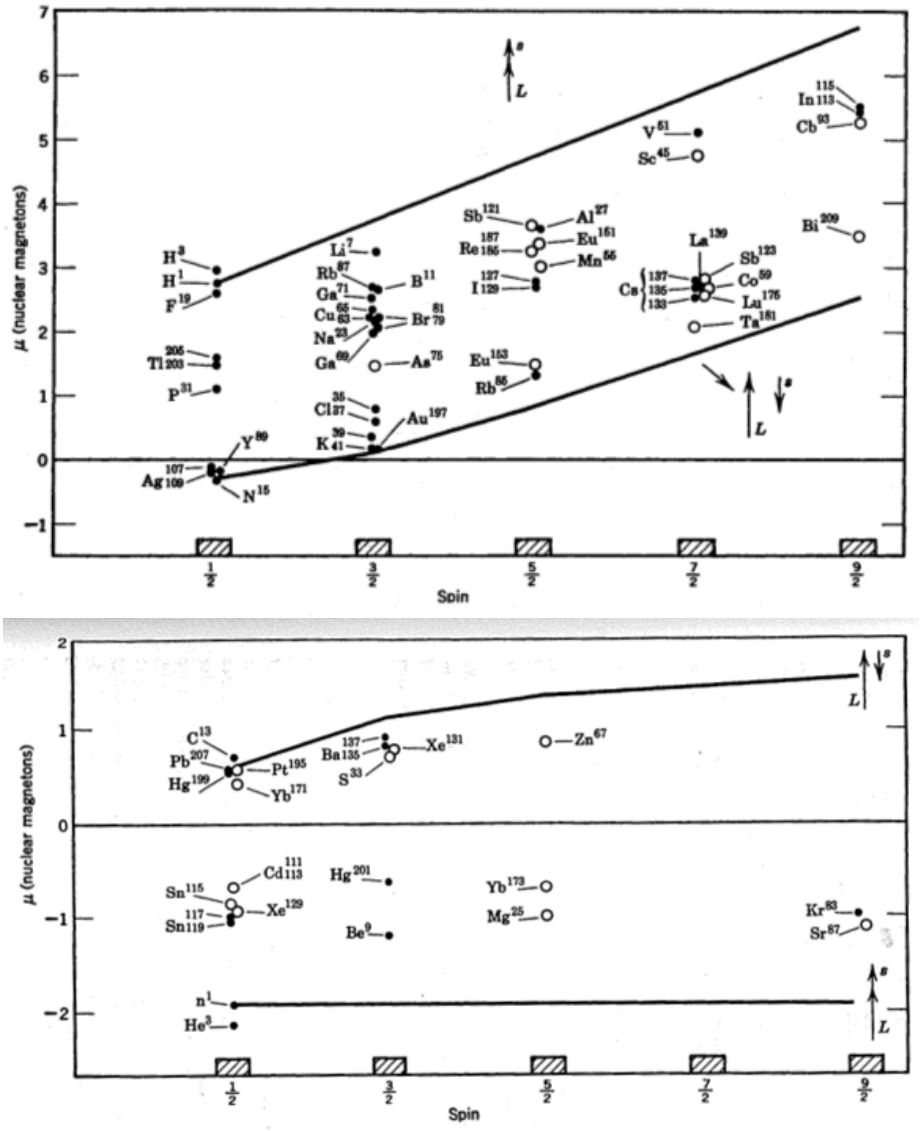

Figure 3.6: Calculated Schmidt lines for magnetic moments as a function of angular momentum J, compared with experimental data. (Figures taken from Blatt and Weisskopf [2])

3.5.3 Isomers

An isomer is a long-lived excited state of a nucleus. (The name comes from an analogy with chemistry in which two chemicals with the same chemical formula can have different properties based on their geometric structure.) Isomers typically occur when the rate for γ-decay is suppressed for some reason, typically a large difference between the spins of the isomeric state and the ground state. Again looking at Figure 3.2, for odd-N nuclei with $N \lesssim 50$ we anticipate low-lying states of $1/2^-$ and $9/2^+$, corresponding to unpaired $1p_{1/2}$ and $0g_{9/2}$ neutrons, respectively. We can predict that isomers might arise in this region because the lowest-multipolarity electromagnetic transition between these two states is E4, or electric hexadecapole. For example, ${}^{85}_{36}\mathrm{Kr}_{49}$ has a $9/2^+$ ground state, and a $1/2^-$ first excited state at 305 keV with a half-life of 4.5 hours. ${}^{87}_{38}\mathrm{Sr}_{49}$ has a $1/2^-$ at 386 keV with a half-life of 2.8 hours. ${}^{71}_{30}\mathrm{Zn}_{41}$ has a $1/2^-$ at 158 keV with a half-life of 4.0 hours.

3.6 Exercises

1. Evaluate the spin orbit force $-V_{\ell s}\vec{\ell}\cdot\vec{s}$, where $V_{\ell s}$ is a scalar coefficient, for a single particle in an orbit with $j = \ell \pm s$. How does the spin-orbit splitting depend on ℓ? Hint: use $j^2 = \ell^2 + s^2 + 2\vec{\ell}\cdot\vec{s}$.

2. Looking at the splitting in ${}^{17}\mathrm{O}$ between the $5/2^+$ ground state and first $3/2^+$ state at 5085 keV, estimate the coefficient $V_{\ell s}$ for the $0d$ orbits. Repeat for the $1p$ orbits in ${}^{41}\mathrm{Ca}$, using the $3/2^-$ state at 1943 keV and the $1/2^-$ state at 3614 keV. Are the results consistent?

Chapter 4

Multiple particles

If we want to describe anything aside from the ground state (and some selected excited states) of odd-A nuclei, the possibilities quickly become richer because we cannot simply treat the particles as moving in a mean field potential. We must additionally treat the residual interaction between valence particles.

For example, if we want to know the ground state of ^{18}F, we could reasonably expect that the valence proton and neutron will sit in their respective $0d_{5/2}$ orbits. However, two distinguishable particles with $j = 5/2$ can couple to $J = 0, 1, 2, 3, 4, 5$, so the IPM would predict a six-fold degenerate ground state with energy $E = \epsilon_{\pi d_{5/2}} + \epsilon_{\nu d_{5/2}}$. This degeneracy is broken by the residual interaction between the two particles. As a first attempt at understanding odd-odd nuclei, we consider the Nordheim rules.

4.1 The Nordheim Rules

The IPM allows us to predict properties of odd-mass nuclei. Can we say something about odd-odd nuclei (with unpaired protons and neutrons)? The empirical *Nordheim rules* give a prediction for the ground-state spin of odd-odd nuclei.

$$\begin{array}{lccc} \text{Strong Nordheim rule:} & J = |j_n - j_p| & (j_n - \ell_n + j_p - \ell_p) & \text{even} \\ \text{Weak Nordheim rule:} & |j_n - j_p| < J \leq j_n + j_p & (j_n - \ell_n + j_p - \ell_p) & \text{odd} \end{array} \tag{4.1}$$

where in the weak rule there is a tendency towards $J = j_p + j_n$. Some examples are given in Table 4.1.

Can we understand why the Nordheim rules might work? (Actually, they don't work all that well.) The quantity $(j_p - \ell_p + j_n - \ell_n)$ is odd if ℓ and s are aligned or anti-aligned for both particles, while it is even if they are aligned for one and anti-aligned for the other. We know from the ground state of the deuteron that the $S = 1, T = 0$ (isoscalar pairing) channel is the most attractive in the proton-neutron channel, and so we may expect that the ground state of odd-odd nuclei are those in which the spins of the proton and neutron are

Table 4.1: Selected ground state spins and their Nordheim rule predictions.

Nuclide	proton orbit	neutron orbit	Nordheim rule	J^π_{gs}
${}^{16}_{7}\mathrm{N}_9$	$0p_{1/2}$	$0d_{5/2}$	Strong: $J = 2$	2^-
${}^{42}_{19}\mathrm{K}_{23}$	$0d_{3/2}$	$0f_{7/2}$	Strong: $J = 2$	2^-
${}^{66}_{29}\mathrm{Cu}_{37}$	$1p_{3/2}$	$0f_{5/2}$	Strong: $J = 1$	1^+
${}^{14}_{7}\mathrm{N}_9$	$0p_{1/2}$	$0p_{1/2}$	Weak: $0 < J \leq 1$	1^+
${}^{18}_{9}\mathrm{F}_9$	$0d_{5/2}$	$0d_{5/2}$	Weak: $0 < J \leq 5$	1^+
${}^{28}_{13}\mathrm{Al}_{15}$	$0d_{5/2}$	$1s_{1/2}$	Weak: $2 < J \leq 3$	3^+

aligned. In the even case, the spins will be aligned if the total angular momenta are anti-aligned, i.e. $J = |j_p - j_n|$, which is reflected in the strong Nordheim rule. In the odd case, the spins will be aligned if the j's are aligned i.e. $J = j_p + j_n$, and this is reflected in the weak rule. As we can see from ^{18}F, the weak rule is not terribly predictive. This is primarily because the rules neglect the effects of configuration mixing.

4.2 Slater-Condon Rules

We now begin to treat the residual interaction between nucleons in a more sophisticated and general way. In principle, when evaluating an operator between two many-body Slater-determinants, one should evaluate a $3A$-dimensional integral over antisymmetrized products of single-particle states:

$$\left\langle \Psi_f \middle| \hat{\mathcal{O}} \middle| \Psi_i \right\rangle = \int d^3r_1 \dots d^3r_A \mathcal{A} \left[\phi^*_{f1}(\vec{r}_1) \dots \phi^*_{fA}(\vec{r}_A) \right] \hat{\mathcal{O}} \mathcal{A} \left[\phi_{i1}(\vec{r}_1) \dots \phi_{iA}(\vec{r}_A) \right]. \tag{4.2}$$

If we have a one-body operator, then it can change at most one orbit, and it can transform

$$|\Psi_i\rangle = \mathcal{A} \left[\phi_1(\vec{r}_1) \dots \phi_q(\vec{r}_q) \dots \phi_A(\vec{r}_A) \right] \tag{4.3}$$

into

$$|\Psi_f\rangle = \mathcal{A} \left[\phi_1(\vec{r}_1) \dots \phi_p(\vec{r}_p) \dots \phi_A(\vec{r}_A) \right] \tag{4.4}$$

and in this case

$$\left\langle \Psi_f \middle| \hat{\mathcal{O}}^{(1)} \middle| \Psi_i \right\rangle = \left\langle \phi_p \middle| \hat{\mathcal{O}}^{(1)} \middle| \phi_q \right\rangle = \int d^3r_m \phi^*_q(\vec{r}) \hat{\mathcal{O}}^{(1)}(\vec{r}) \phi_p(\vec{r}). \tag{4.5}$$

If more than one orbit it changed between $|\Psi_i\rangle$ and $|\Psi_f\rangle$, then the matrix element is zero. If $|\Psi_i\rangle = |\Psi_f\rangle$, then the matrix element is the sum of diagonal one-body terms of $\hat{\mathcal{O}}^{(1)}$

$$\left\langle \Psi \middle| \hat{\mathcal{O}}^{(1)} \middle| \Psi \right\rangle = \sum_p \left\langle \phi_p \middle| \hat{\mathcal{O}}^{(1)} \middle| \phi_p \right\rangle. \tag{4.6}$$

Similarly, for a two-body operator if the initial and final states differ by two particles then

$$\left\langle \Psi_f \middle| \hat{\mathcal{O}}^{(2)} \middle| \Psi_i \right\rangle = \left\langle \phi_p \phi_q \middle| \hat{\mathcal{O}}^{(2)} \middle| \phi_r \phi_s \right\rangle - \left\langle \phi_p \phi_q \middle| \hat{\mathcal{O}}^{(2)} \middle| \phi_s \phi_r \right\rangle. \tag{4.7}$$

The second term with the minus sign comes from the antisymmetrization $\mathcal{A}$ (recall that this includes a normalization factor $1/\sqrt{A!}$). We can see this for a two-particle wave function

$$\begin{array}{ll} |\Psi_i\rangle = \mathcal{A}\left[\phi_p \phi_q\right] & = \frac{1}{\sqrt{2!}} \left(\phi_p \phi_q - \phi_q \phi_p\right) \\ |\Psi_f\rangle = \mathcal{A}\left[\phi_r \phi_s\right] & = \frac{1}{\sqrt{2!}} \left(\phi_r \phi_s - \phi_s \phi_r\right) \end{array} \tag{4.8}$$

and

$$\begin{aligned} \left\langle \Psi_f \middle| \mathcal{O}^{(2)} \middle| \Psi_f \right\rangle &= \frac{1}{2} \int dr_1 dr_2 \left(\phi_p^* \phi_q^* - \phi_q^* \phi_p^*\right) \mathcal{O}^{(2)} \left(\phi_r \phi_s - \phi_s \phi_r\right) \\ &= \int dr_1 dr_2 \left(\phi_p^* \phi_q^*\right) \mathcal{O}^{(2)} \left(\phi_r \phi_s\right) - \int dr_1 dr_2 \left(\phi_p^* \phi_q^*\right) \mathcal{O}^{(2)} \left(\phi_s \phi_r\right) \end{aligned} \tag{4.9}$$

4.3 Two-body matrix elements

When dealing with the residual interaction between valence particles, we consider the quantity

$$\langle ab|V|cd\rangle \equiv \int d^3 r_1 d^3 r_2 \phi_a^*(\vec{r}_1) \phi_b^*(\vec{r}_2) V(\vec{r}_1 - \vec{r}_2) \phi_c(\vec{r}_1) \phi_d(\vec{r}_2) \tag{4.10}$$

which is called a *two-body matrix element* (TBME). This gives the amplitude for two particles in single-particle orbits ϕ_c and ϕ_d to scatter via the potential V into single-particle orbits ϕ_a and ϕ_b. Here, a is a shorthand label for the set of quantum numbers $(n_a, \ell_a, j_a, m_a, t_{za})$. In second-quantized notation with non-antisymmetrized matrix elements, the operator may be expressed as

$$\hat{V} = \frac{1}{2} \sum_{abcd} \langle ab|V|cd\rangle a_a^\dagger a_b^\dagger a_d a_c. \tag{4.11}$$

At this point, our two-body states are constructed by a product of two single-particle states.

$$|ab\rangle = |a\rangle|b\rangle \tag{4.12}$$

Since we know that the full A-body wave function must be anti-symmetric under the exchange of two particles, we can re-write the TBME in terms of an anti-symmetric two-body basis

$$|ab\rangle^{\mathcal{A}} = \frac{1}{\sqrt{2}}(|a\rangle|b\rangle - |b\rangle|a\rangle). \tag{4.13}$$

We can see now that $|ab\rangle^{\mathcal{A}} = -|ba\rangle^{\mathcal{A}}$, and that $|ba\rangle = 0$ if $a = b$, and so Fermi statistics are respected. The antisymmetrized TBME is then

$$\langle ab|V|cd\rangle^{\mathcal{A}} = \frac{1}{2}(\langle ab|V|cd\rangle - \langle ba|V|cd\rangle - \langle ab|V|dc\rangle + \langle ba|V|dc\rangle) \tag{4.14}$$

By looking at (4.10), we can see that $\langle ab|V|cd\rangle = \langle ba|V|dc\rangle$ (simply re-label the dummy integration variables), and likewise with the other two terms, so we have

$$\langle ab|V|cd\rangle^{\mathcal{A}} = \langle ab|V|cd\rangle - \langle ab|V|dc\rangle \tag{4.15}$$

and the operator may be written in terms of anti-symmetrized matrix elements as

$$\hat{V} = \frac{1}{4}\sum_{abcd}\langle ab|V|cd\rangle^{\mathcal{A}} a_a^\dagger a_b^\dagger a_d a_c. \tag{4.16}$$

The factor $\frac{1}{4}$ arises because we sum freely over the four indices, and so over-count by a factor of 4.

So far, we have considered a two-body state in which each of the particles has a good angular momentum projection m. This is called an *M-scheme* basis. We can equivalently consider a basis in which the particles are coupled to good total angular momentum J (called *J-scheme*). If the Hamiltonian is spherically symmetric, then the interaction will not depend on the projection M of J, and we can drop the M quantum number when working in J-scheme. The two bases are related by a Clebsch-Gordan coefficient (this is what Clebsch-Gordan coefficients were born to do)

$$|ab\rangle_{JM} = \sum_{m_a m_b}\langle j_a m_a, j_b m_b|JM\rangle|ab\rangle.^{1} \tag{4.17}$$

and the anti-symmetrized ket is

$$|ab\rangle_{JM}^{\mathcal{A}} = \frac{1}{\sqrt{1+\delta_{ab}}}\sum_{m_a m_b}\langle j_a m_a, j_b m_b|JM\rangle|ab\rangle^{\mathcal{A}} \tag{4.18}$$

If we assume spherical symmetry for the core (which is reasonable for a doubly-magic nucleus), then the residual interaction will not depend on the projection of the total angular momentum M. This fact leads to a significant reduction in storage requirements for codes implemented in J-scheme (however, it also incurs the burden of angular momentum algebra).

As an example, we consider the energy of the first $J^\pi = 5^+$ state in ^{18}F. We treat ^{18}F as a valence proton and a valence neutron on top of a doubly-magic ^{16}O core. We further assume that the low-lying states are dominated by configurations in which both particles are in the $1s0d$ shell. In this case, there is only one configuration which can form a 5^+ state – namely one in which both the proton and neutron are in their respective $0d_{5/2}$ orbits, and their angular momenta are coupled to $J = 5$.

[1] There is some risk of confusion here due to the notation. On the left-hand side, a now refers to the quantum numbers $(n_a, \ell_a, j_a, t_{za})$ – it no longer includes m_a. This should be clear by the subscript indicating that the ket is coupled to good total J, and thus cannot in general have well-defined m_a and m_b.

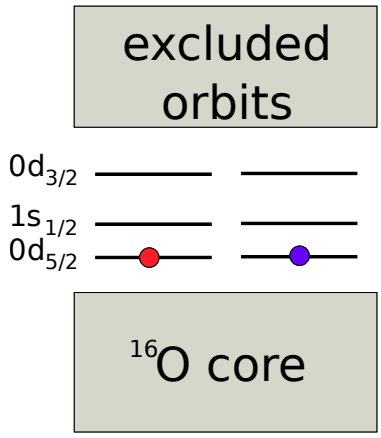

Figure 4.1: A simple shell-model picture of the lowest 5^+ state in ^{18}F.

The energy of that state is then given by the energy of the ^{16}O core, plus the single-particle energies of each valence nucleon, plus the residual interaction.

$$E(^{18}\mathrm{F}; 5^+) = E(^{16}\mathrm{O}) + \epsilon_{\pi d_{5/2}} + \epsilon_{\nu d_{5/2}} + \left\langle \pi d_{5/2} \nu d_{5/2} \middle| V \middle| \pi d_{5/2} \nu d_{5/2} \right\rangle_{J=5} \quad (4.19)$$

Here I have introduced the notation of π to indicate proton orbits and ν to indicate neutron orbits. [2] The energy of the ^{16}O ground state is -127.619 MeV. We can take the single-particle energies from the one-neutron and one-proton separation energies of ^{17}O and ^{17}F, respectively. These give $\epsilon_{\nu d_{5/2}} = -4.143$ MeV, and $\epsilon_{\pi d_{5/2}} = -0.600$ MeV. We take the TBME from the USDB interaction, which gives $\left\langle \pi d_{5/2} \nu d_{5/2} \middle| V \middle| \pi d_{5/2} \nu d_{5/2} \right\rangle_{J=5} = -4.321$ MeV.[3] Putting these together, we have $E(^{18}F; 5^+) = -136.683$ MeV, which may be compared with the experimental value of -136.248.

4.4 Pairing and Seniority

One of the few universal facts about nuclear structure is that all even-even nuclei have a ground-state spin-parity of 0^+. This finding is of great importance for the IPM, because it allows us to predict the properties of odd-mass nuclei by only considering the odd nucleon.

The essential explanation of this fact, given by Mayer, is that pairs of nucleons tend to pair off to spin 0. To understand why, we consider the facts that the nuclear interaction is generally attractive and short-ranged. For computational ease, we assume a schematic delta interaction $V = -g\delta(\vec{r})$, where g is a positive

[2] In isospin representation, since we have identical orbits we require $(-1)^{J+T}$ to be odd, and since $J = 5$, we take $T = 0$.

[3] A microscopic interaction obtained with in-medium SRG (discussed later) using NN + 3N interactions from chiral effective field theory yields -4.349 MeV

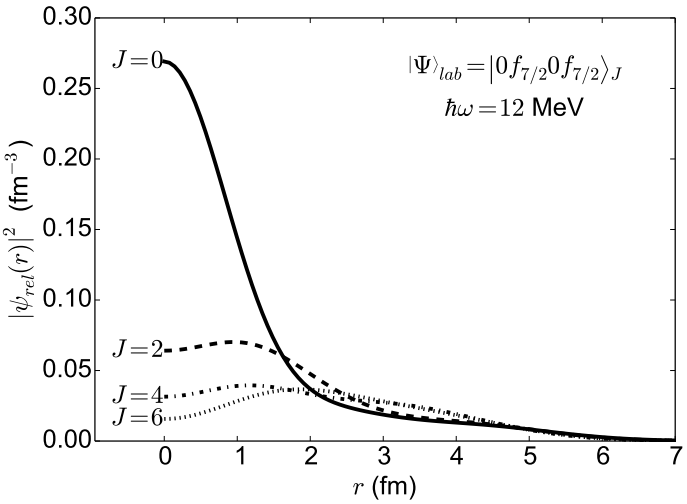

Figure 4.2: The probability density as a function of relative distance r for two identical nucleons in $0f_{7/2}$ orbits, coupled to a given J, evaluated in a harmonic oscillator basis with $\hbar\omega$=12 MeV. The strong peak for small r at $J = 0$, coupled with an attractive short-range potential, provides an explanation for the pairing phenomenon.

constant, so that the potential is attractive. In the relative coordinates with spherical symmetry, we then have

$$\begin{aligned} \langle\psi|V|\psi\rangle &= -g \int dr \psi^*_{rel}(r)\delta(r)\psi_{rel}(r) \\ &= -g\,|\psi_{rel}(0)|^2 \end{aligned} \tag{4.20}$$

The only remaining trouble is that in the shell model we are used to working with *lab-frame* coordinates, while this simple form is in *relative* coordinates. We may, of course, transform between the two. The easiest basis (by far) in which to perform the transformation is the harmonic oscillator basis. The procedure involves some angular momentum recoupling and what are called Moshinsky oscillator brackets, which will mercifully not be discussed here. The result is shown in Figure 4.2, which presents the probability density $|\psi_{rel}(r)|^2$ as a function of the relative coordinate for two identical $0f_{7/2}$ nucleons coupled to $J = 0, 2, 4, 6$ (odd J is forbidden by the Pauli principle).

A clear analogy may be made with the BCS theory of superconductivity, which shows that the formation of Cooper pairs will become energetically favorable for orbits near the Fermi surface if the residual interaction between particles is attractive. The pairing gap Δ_k is given, in a notation suitable for a

condensed-matter system, by (see, e.g. [9])

$$\Delta_k = \sum_{k'} \langle k - k|V|k' - k'\rangle u_{k'} v_{k'} \tag{4.21}$$

where k labels momentum states, and $u_{k'}, v_{k'}$ are coefficients which transform the BCS Hamiltonian to a diagonal form. The equivalent gap in our notation would be $\Delta = \langle aa|V|bb\rangle_{J=0}$.

The presence of the pairing gap suggests a scheme for categorizing multi-particle configurations. For a given configuration of n nucleons, we assign an additional quantum number v, called the *seniority*, which counts the number of unpaired nucleons. From the preceding discussion, we would expect that a lower seniority state will have lower energy, due to the pairing gap. In the limit that pairing is the dominant interaction between nucleons, seniority becomes a good quantum number – the Hamiltonian cannot break a pair – and excited states of a given seniority are degenerate.

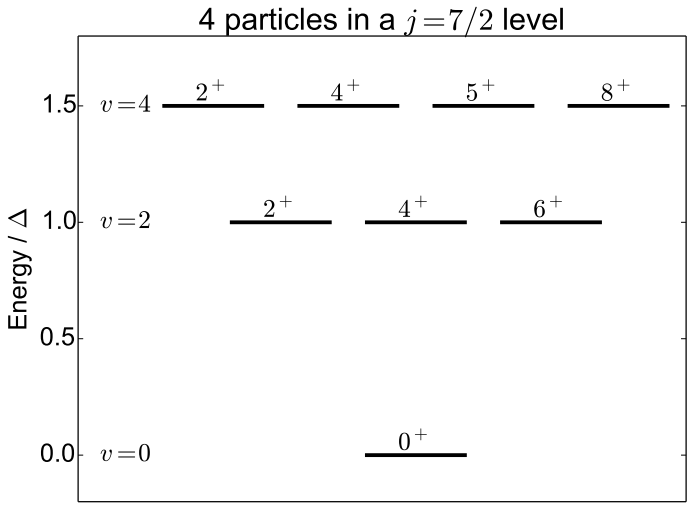

Figure 4.3: Spectrum of states of four particles in a $j = 7/2$ orbit in the limit of a pure pairing interaction.

As an illustration of this, we consider four neutrons in the $0f_{7/2}$ orbit in the extreme pairing limit. The only state we can construct with $v = 0$ is a 0^+ state, which should be the ground state. At $v = 2$ (note that we can't get $v = 1$, since if we break a pair we have two unpaired neutrons), the unpaired neutrons can couple to $J = 2, 4, 6$, which should be degenerate excited states with energy Δ. At $v = 4$, we can generate a states with $J = 2, 4, 5, 8$ which should have energy 2Δ. Actually, if we would treat the pairing problem carefully [9], we would find

that the energy difference between levels of different parity is given by

$$E_{v+2} - E_v = \Delta(1 + \frac{2v}{2j+1}) \tag{4.22}$$

where j is the angular momentum of the orbit.

The classic example of pairing in nuclei is the tin isotopes ($Z = 50$), where the 2^+ energy is approximately constant from $A = 102$ to $A = 128$. This energy can be understood as the energy to break a pair of neutrons, and is thus independent of A. The energy of the 2+ is lower than that of higher J due to configuration mixing, which will be discussed in the next chapter.

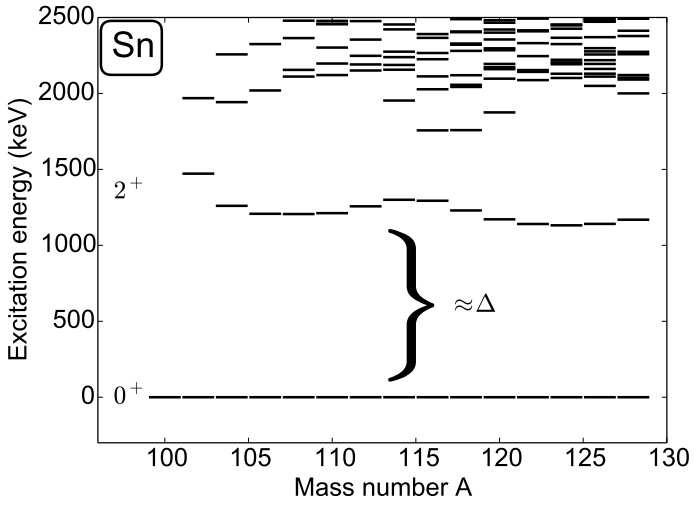

Figure 4.4: Energies of the tin isotopes, displaying a nearly-constant 2^+ excitation energy across almost 30 mass units.

4.5 Monopole interaction and effective single-particle energies

As we fill a major shell, the positions of single-particle levels – at the level of the IPM – will change, as the effective mean field changes. The dominant effect of filling a subshell is given by the angle-averaged, or *monopole* component of the interaction.

$$\bar{V}_{ab} = \frac{\sum\limits_{m_a m_b} \langle am_a bm_b|V|am_a bm_b\rangle}{\sum\limits_{m_a m_b} 1} = \frac{\sum\limits_J (2J+1)\langle ab|V|ab\rangle_J}{\sum\limits_J (2J+1)} \tag{4.23}$$

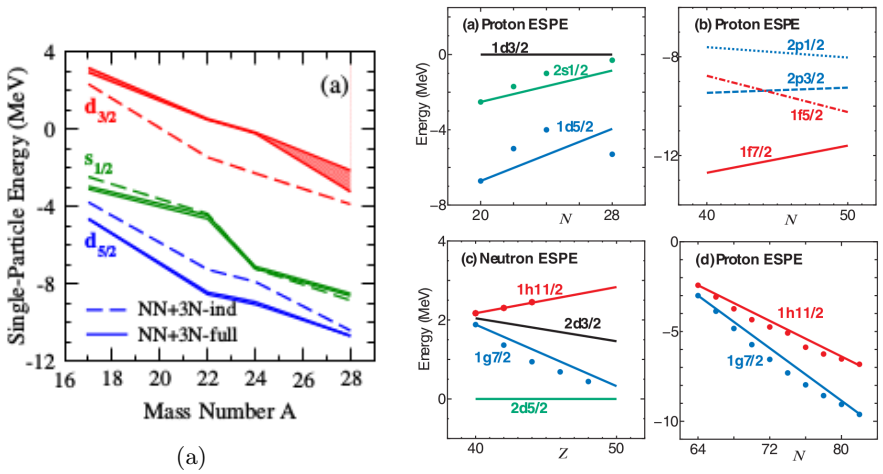

(a) (b)

Figure 4.5: Evolving single-particle energies as a function of mass number A, taken from (a) Bogner et al. PRL 113 142 501 (2014) and (b) Otsuka et al PRL 95 232502 (2005). Shamelessly reproduced without permission.

If the orbit j_a is filled, i.e. its occupation goes from 0 to $2j_a + 1$, then the change in energy of a particle in orbit j_b will be given by $(2j_a + 1)\bar{V}_{ab}$. The monopole is frequently used when discussion the evolution of shell structure along an isotopic or isotonic chain. In figure 4.5(a), the evolution of the neutron single particle energies as neutrons are added to the *sd*-shell is used to explain the oxygen dripline. In figure 4.5(b), the evolution of single-particle orbits leads to new shell gaps.

4.6 Exercises

1. Derive the normalization factor given in equation (4.18).
2. Prove the second equality in equation (4.23).
3. By enumerating possible M-scheme states, show that for two particles in a $j = 7/2$ shell, the allowed values of J are 0,2,4,6. Next, show that for four particles in a $j = 7/2$ shell, the allowed J values are 0,2,4,5,6,8, with two $J = 2$ and $J = 4$ states.

Chapter 5

Interacting shell model

In general, the many-body states we are considering will not be well-described by a single Slater determinant (configuration). There will be some coupling between the different configurations, which will lead to configuration mixing. The simplest example of this is two-level mixing, which I will briefly discuss as a reminder.

Consider a system with an unperturbed Hamiltonian H_0 with eigenstates $|\phi_1\rangle$ and $|\phi_2\rangle$ and respective energies ϵ_1,ϵ_2. If we add a perturbing interaction V which couples the eigenstates $\langle\phi_2|V|\phi_1\rangle = \Delta$, then the Hamiltonian may be expressed as

$$H = H_0 + V = \begin{pmatrix} \epsilon_1 & \Delta \\ \Delta & \epsilon_2 \end{pmatrix} \tag{5.1}$$

The actual ground and excited states $|\psi_1\rangle$ and $|\psi_2\rangle$ are the eigenvectors of this perturbed Hamiltonian. In this case, the resulting eigenstates and eigenvalues are

$$\begin{aligned} |\psi_1\rangle &= \cos\theta|\phi_1\rangle - \sin\theta|\phi_2\rangle \quad , \quad E_1 = \epsilon_1\cos^2\theta + \epsilon_2\sin^2\theta - 2\Delta\sin\theta\cos\theta \\ |\psi_2\rangle &= \cos\theta|\phi_2\rangle + \sin\theta|\phi_1\rangle \quad , \quad E_2 = \epsilon_2\cos^2\theta + \epsilon_1\sin^2\theta + 2\Delta\sin\theta\cos\theta \end{aligned} \tag{5.2}$$

with the angle θ defined by $\tan\frac{\theta}{2} = \frac{2\Delta}{\epsilon_2-\epsilon_1}$.

We can see that the mixing between the two states will be maximized if the strength of the perturbation Δ is large compared to the original energy difference. If on the other hand, the perturbation is small compared to the original energy difference, then we may ignore that mixing, to some approximation. This motivates and justifies the interacting shell model picture. In this approach, the gaps in single-particle energies associated with the magic numbers allows us to explicitly treat mixing in a small *valence space*, while neglecting the mixing outside of the valence space.

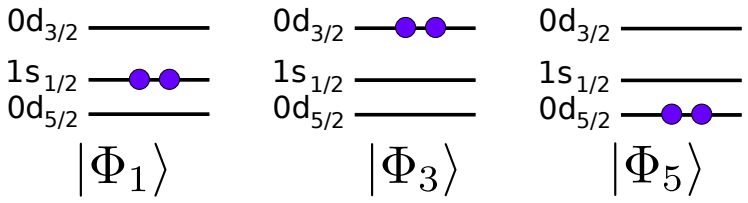

Figure 5.1: *sd* configurations for ^{18}O with $J^\pi = 0^+$.

5.1 Valence space diagonalization

We now turn to the case of the ground state of ^{18}O. Naively, we would consider the shell model wave function to be $\left|0d_{5/2}0d_{5/2}\right\rangle_{J=0}$, and we would proceed as we did for the 5^+ state in ^{18}F. However, within the *sd* shell, we have two additional 0^+ states given by $\left|1s_{1/2}1s_{1/2}\right\rangle_{J=0}$ and $\left|0d_{3/2}0d_{3/2}\right\rangle_{J=0}$, as shown in Figure 5.1, and we should consider the coupling between them. If we have single-particle energies ϵ_1,ϵ_3, ϵ_5, and interaction matrix elements $\left\langle 0s_{1/2}0s_{1/2}\right|V\left|0d_{5/2}0d_{5/2}\right\rangle_{J=0} = v_{15}$, etc, then the *sd* shell Hamiltonian for $J^\pi = 0^+$ may be written in matrix form as

$$H(0^+) = \begin{pmatrix} 2\epsilon_1 + v_{11} & v_{13} & v_{15} \\ v_{13} & 2\epsilon_3 + v_{33} & v_{35} \\ v_{15} & v_{35} & 2\epsilon_5 + v_{55} \end{pmatrix}. \tag{5.3}$$

The task is thus to diagonalize this 3×3 matrix. This is painful to do symbolically, but can be done easily numerically. We take the values for the Hamiltonian from the USDB interaction (shown in Table 5.1). Diagonalizing the 3×3 matrix we obtain eigenvalues and eigenvectors

$$\begin{array}{lllllllll} E_1 & = -11.932 & , & |\psi_1\rangle = & 0.418|\Phi_1\rangle & + & 0.221|\Phi_3\rangle & + & 0.881|\Phi_5\rangle \\ E_2 & = -7.339 & , & |\psi_2\rangle = & 0.907|\Phi_1\rangle & - & 0.04|\Phi_3\rangle & - & 0.42|\Phi_5\rangle\,. \\ E_3 & = 3.077 & , & |\psi_3\rangle = & 0.058|\Phi_1\rangle & - & 0.974|\Phi_3\rangle & + & 0.217|\Phi_5\rangle \end{array} \tag{5.4}$$

Had we ignored the mixing, then we would have obtained $E_1 = -10.411$, $E_2 = -8.107$, $E_3 = 2.324$ – a modest correction. As more particles are added to the valence space, the mixing becomes more important.

5.2 Lanczos algorithm

The dimension of the Hamiltonian matrix can quickly get very large, and so numerical treatment of the problem becomes expensive. In the very common case where we are only interested in the lowest few eigenvalues, then the Lanczos algorithm for matrix diagonalization becomes an attractive choice. The general idea is that if we begin with some random initial vector $\vec{x}$, this may be expressed as a linear combination of the eigenvectors $\vec{v}_i$ of the matrix M.

$$\vec{x}^{(0)} = \sum_i c_i \vec{v}_i \tag{5.5}$$

Table 5.1: $J = 0$, $T = 1$ matrix elements from the USDB interaction. The single particle energies are given by $\epsilon_1 = -3.2079$, $\epsilon_3 = 2.1117$, $\epsilon_5 = -3.9257$.

term	USDB
v_{11}	-1.6913
v_{13}	-1.0150
v_{15}	-1.5602
v_{33}	-1.8992
v_{35}	-3.1025
v_{55}	-2.5598

where the coefficients c_i are unknown. If we now multiply by M, we obtain a new vector $\vec{x}^{(1)}$ given by

$$M\vec{x}^{(0)} = \vec{x}^{(1)} = \sum_i c_i e_i \vec{v}_i \tag{5.6}$$

where e_i are the eigenvalues of M. If we repeat this multiplication n times, then we have

$$M^n\vec{x}^{(0)} = \vec{x}^{(n)} = \sum_i c_i e_i^n \vec{v}_i. \tag{5.7}$$

We can now see that each iteration multiplies the contribution of $\vec{v}_i$ to $\vec{x}^{(n)}$ by e_i. Fairly quickly, the eigenvector with the largest magnitude eigenvalue should dominate $\vec{x}^{(n)}$. Ten, the change between $\vec{x}^{(n)}$ and $\vec{x}^{(n+1)}$ will fall below some tolerance threshold and $\vec{x}^{(n)} \approx \vec{v}_{i_{max}}$. Next, we can construct a new initial vector $\vec{y}^{(0)}$, which is orthogonal to $\vec{x}^{(n)}$, and repeat the procedure, yielding the eigenvector with the next-largest eigenvalue, and continue for as many eigenvectors as are desired.

5.3 Deformation and the emergence of collectivity

In nearly all nuclear structure courses, at least some time is devoted to collective models, most notably vibrational and rotational models. Often, little to no discussion is given on how these models relate to the shell model. I will try to at least make a passing attempt at that here.

5.3.1 Coherent states

In order to illustrate coherence, we consider a 2×2 Hamiltonian matrix.

$$H = \begin{pmatrix} 1 & 1 \\ 1 & 1 \end{pmatrix}. \tag{5.8}$$

To find the eigenvalues and eigenvectors, we solve the characteristic equation

$$(1 - \lambda)^2 - 1 = 0 \tag{5.9}$$

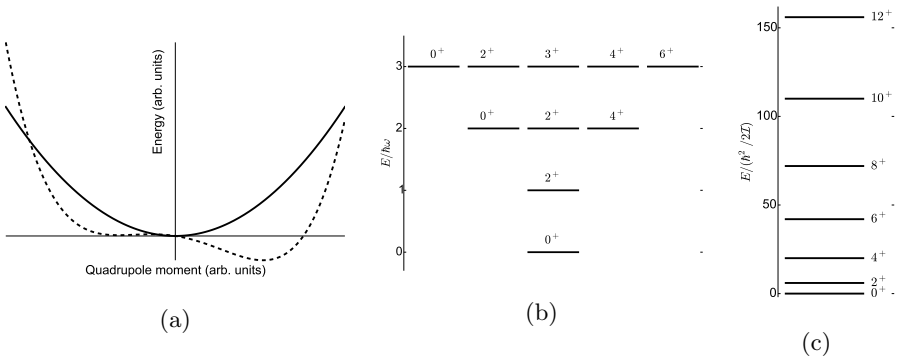

Figure 5.2: (a)Two possible curves showing the energy as a function of quadrupole deformation. (b) A vibrational spectrum. (c) A rotational spectrum.

which yields $\lambda = 0$ and 2 with eigenvalues of $(1, -1)$ and $(1, 1)$, respectively. If we were to solve the equivalent 3×3 matrix, we would obtain eigenvalues $\lambda = 0, 0, 3$ with the last eigenvector being $(1, 1, 1)$. For an $N \times N$ matrix, we would obtain $N - 1$ zeros, and one eigenvalue $\lambda = N$, with eigenvector $(1, 1 \ldots, 1)$. The take home message here is that if we have a system with many degenerate states whose coupling is roughly constant, we obtain one state which is a coherent superposition of the original states, and which drops down or up proportional to the number of states mixing in. This state is called a collective state. The other states remain roughly in the same position. I will now discuss some types of collective excitation.

5.3.2 Collective excitations of nuclei

In a vibrational model, one begins from a liquid drop model and notes the opposing effects of the surface tension and the Coulomb interaction. The surface tension prefers a spherical shape, while Coulomb prefers a deformed shape. If the surface tension wins, the ground state is spherical (see solid curve in Figure 5.2). In this case, for small oscillations in quadrupole moment there is essentially a harmonic potential. We can use the machinery of the quantum harmonic oscillator and obtain a spectrum (neglecting the zero-point energy)

$$E_{vib}(N) = N\hbar\omega \tag{5.10}$$

where N is the number of oscillator quanta (phonons). I will consider here phonons of quadrupole nature which have $J^+ = 2^+$. If we have a one-phonon state, then, it will be a 2^+ excitation. If we have a two-phonon state, the two phonons can couple to $0^+, 2^+, 4^+$, and we have a triplet of states, and so on, resulting in a vibrational spectrum.

In a rotational model, the energy balance is in favor of deformation in the ground state (see the dashed line in Figure 5.2). In this case, spherical symmetry

has been broken, and we may now produce excited states by rotating the nucleus about an axis perpendicular to the axis of symmetry. Beginning with the energy of a classical rotor and taking the quantum limit, we have

$$E_{rot} = \frac{1}{2}\mathcal{I}\omega^2 = \frac{J^2}{2\mathcal{I}} \rightarrow \frac{J(J+1)}{2\mathcal{I}} \tag{5.11}$$

Where $\mathcal{I}$ is the moment of inertia.

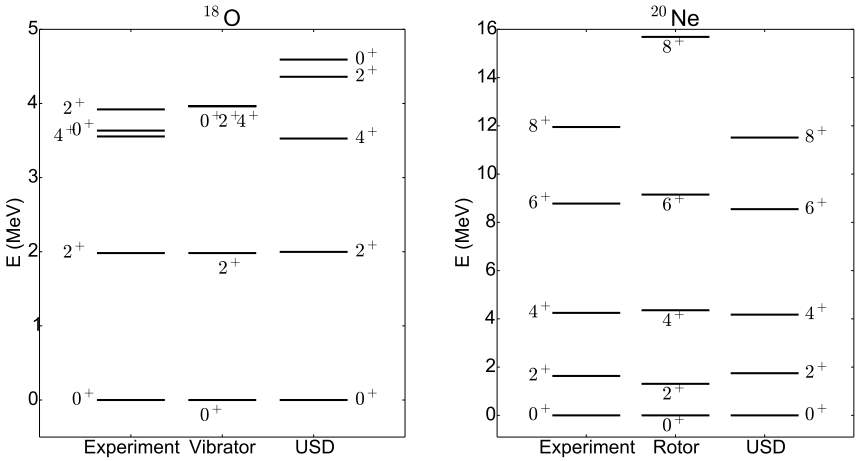

Figure 5.3: Spectra of ^{18}O and ^{20}Ne, compared to collective models and shell model calculations with the USD interaction.

So the question arises (for me at least), what do these collective excitations look like in a shell model picture? One might be tempted to say that these two models are mutually exclusive and describe different phenomena – states that are well-described by a collective model should be outside the realm of the shell model. However, we can see collective behavior even in nuclei that should be (and are) well-described by the shell model; an example is given in Figure 5.3.

5.3.3 Superfluidity

In the last chapter, I discussed pairing and how the short-range nuclear interaction is strongest in the $J = 0$ channel. It turns out that if we make the same plot, but instead consider off-diagonal matrix elements $\langle aa|V|bb\rangle_J$, we see a similar trend. These too are strongly-peaked at short distances for $J = 1$. This means we can approximately write the pairing Hamiltonian as

$$H_{pair} = -\Delta \begin{pmatrix} 1 & 1 & \dots \\ 1 & 1 & \dots \\ \vdots & \vdots & \ddots \end{pmatrix}. \tag{5.12}$$

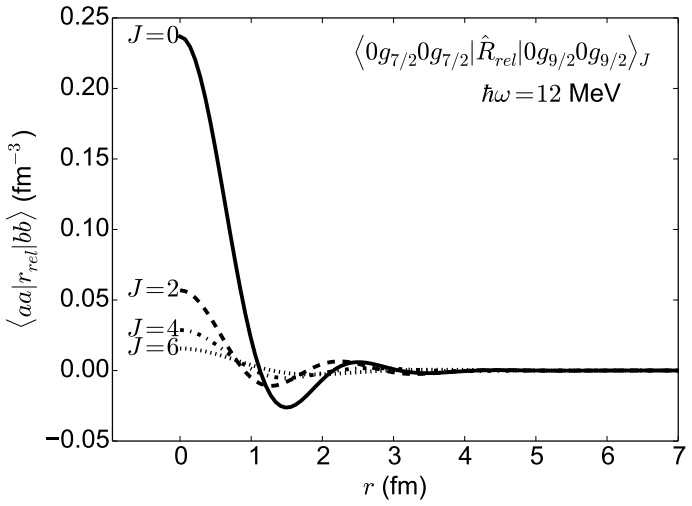

Figure 5.4: Off-diagonal radial overlap of two identical particles.

where the relevant basis is of all $J = 0$ shell model configurations. As we just saw, this leads to one collective state being singled out and lowered in energy relative to the others, by an amount $\sim N\Delta$. This is the superconducting ground state that we see in the tin isotopes.

5.3.4 Vibrations

We now turn to the vibrations of the liquid drop model. Let's consider a quadrupole phonon. We can write the one-phonon state as

$$|\Psi_{1phon}\rangle = \mathcal{Q}^\dagger_\mu(t)|\Psi_{0phon}\rangle \tag{5.13}$$

The phonon creation operator can be written as

$$\mathcal{Q}^\dagger_\mu(t) = \mathcal{N}e^{-i\omega t}\sum_{ia}\langle i|Q_\mu|a\rangle a^\dagger_i a_a \tag{5.14}$$

where $\hbar\omega$ is the energy of the one-phonon state, $Q_\mu = r^2Y^2_\mu$ is the quadrupole operator [1], $\mathcal{N}$ is a normalization constant and i runs over unoccupied states while a runs over occupied states. Note that if we have many available states, then the normalization factor becomes small, and the contribution of each individual excitation shrinks.

[1] modulo some numerical constant which we will ignore for now.

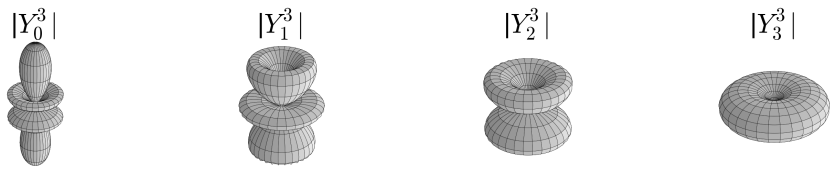

Figure 5.5: Absolute values of the $\ell = 3$ spherical harmonics

The vibrator Hamiltonian is

$$\begin{aligned} H_{vib} = \hat{N}\hbar\omega &= \mathcal{Q}_\mu^\dagger \mathcal{Q}_\mu \hbar\omega \\ &= \mathcal{N}^2\hbar\omega \sum_{ijkl} \langle i|Q_\mu|a\rangle\langle b|Q_{-\mu}|j\rangle a_i^\dagger a_a a_b^\dagger a_j \\ &= \mathcal{N}^2\hbar\omega \left(\sum_{ij} \langle i|Q_\mu|a\rangle\langle a|Q_{-\mu}|j\rangle a_i^\dagger a_j + \sum_{ijab} \langle i|Q_\mu|a\rangle\langle b|Q_{-\mu}|j\rangle a_i^\dagger a_b^\dagger a_j a_a \right). \end{aligned} \tag{5.15}$$

Schematic quadrupole-quadrupole interactions of this nature are frequently used in theoretical investigations of collective phenomena. To the extent that the nucleon-nucleon interaction approximates this Hamiltonian, the nucleus will have a vibrational spectrum. Note that within a boson model, we could add an infinite number of phonons. However, since these approximate bosons are made of fermions, at some point the excited states get Pauli blocked and the harmonic model breaks down.

5.3.5 Rotations

Now we move to rotations, which require a statically-deformed ground state. How does a static deformation occur in the shell model?

We begin with a spherical closed-shell nucleus and add a neutron. We define the z axis so that the neutron is in the $m = j$ state. We now add a second neutron. Due to the effect of pairing, the lowest-energy state will be the one with $m = -j$, so that they couple to $J = 0$. Considering the $m_\ell = \pm\ell$ spherical harmonics, the spatial distribution of both neutrons will be spread out in the x-y plane, resulting in an overall oblate shape (see Figure 5.5). The next neutron we add will be Pauli blocked from occupying a maximal-overlap state, so it takes the next best orbit, which still adds somewhat to the deformation (assuming $j > 3/2$). On the other hand, we can add two more protons in the $m = \pm j$ orbits, leading to an approximate doubling of the quadrupole moment. For this reason, deformation is enhanced when there are both valence protons and valence neutrons.

One can show [4, 9], that the expected quadrupole moment for an odd number N of particles in a single j shell – assuming all pairs of nucleons couple to

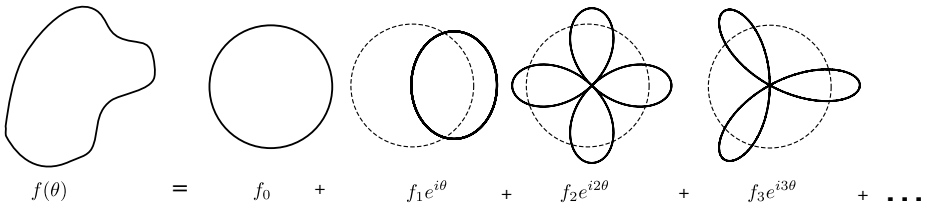

$J = 0$ – is given by

$$\langle j^N j \| Q \| j^N j \rangle = -\frac{2j + 1 - 2N}{2j + 1} \langle r^2 \rangle. \tag{5.16}$$

The quadrupole moment starts out as negative (i.e. oblate), crosses through zero when the shell is half filled ($2N = 2j + 1$), and ends up positive (i.e. prolate) before the shell is totally filled. If there is another subshell nearby, it may be energetically favorable for the next nucleon to jump to the next shell before the lower one is filled, due to the gain in overlap energy.

For even-even nuclei, the deformed ground state has $J^\pi = 0^+$, which requires spherical symmetry, in seeming contradiction with our assumed deformation. The resolution to this predicament is that the symmetry axis of the deformed nucleus picks out a particular direction. But any direction is equally acceptable. In fact the ground state is a superposition of all directions. The first 2^+ state, on the other hand, has a direction.

It's easier to first think of what happens in a two-dimensional system and then generalize to 3D. Consider some shape on the page, described by $f(\theta)$. This shape is the 2D analog of our deformed intrinsic-frame nucleus. We may perform a *partial wave decomposition* of the function $f(\theta)$ – essentially the polar equivalent of a Fourier transform – writing

$$f(\theta) = \sum_{m=0}^{\infty} f_m e^{im\theta}. \tag{5.17}$$

We have now decomposed $f(\theta)$ into component which each have a well-defined angular momentum m. To pick out one of these components, we can multiply by $e^{-im\theta}$ and integrate:

$$f_m = \int_0^{2\pi} d\theta e^{im\theta} f(\theta). \tag{5.18}$$

To move to three dimensions, we replace the $e^{im\theta}$ with a Wigner D matrix $\mathcal{D}^J_{MK}$ where K is the projection of the symmetry axis on the J axis. For $K = 0$ $\mathcal{D}$ reduces to a spherical harmonic.

The rotational wave function can be written as [4]

$$|\Psi_{KJM}\rangle = \mathcal{N} \left(\mathcal{D}^J_{MK} |\Phi_K\rangle + (-1)^{J+K} \mathcal{D}^J_{M-K} |\Phi_{\bar{K}}\rangle \right) \tag{5.19}$$

where $|\Phi_K\rangle$ is the *intrinsic* wave function with angular momentum projection K onto the J axis. The two terms come from the fact that clockwise and counter-clockwise rotations are degenerate and we must construct a superposition of the

two. In the simplest case $K = 0$, which corresponds to the ground state band of even-even nuclei, the $\mathcal{D}$ functions reduce to spherical harmonics. Additionally the above expression collapses to a single term with the restriction to even J:

$$|\Psi_{0JM}\rangle = \mathcal{N} Y^J_M |\Phi_{K=0}\rangle \tag{5.20}$$

In all these cases, we can think of the $\mathcal{D}^J_{MK}$ function as a projection onto a state with good anglular momentum J. So in this light, the rotational states are the different J components of the intrisic deformed state $|\Phi_K\rangle$. Further discussion of rotational structures within the shell model typically relies heavily on group theory and will not be discussed here.

5.4 Practicalities

5.4.1 The center of mass problem

Out of convenience, shell model calculations are performed in the lab-frame. However, we are generally interested only in the relative degrees of freedom. The center of mass motion is trivial. The nice feature about using an oscillator basis is that it may be factored into relative and center-of-mass coordinates.

$$H = \frac{1}{2m}(p_1^2 + p_2^2) + \frac{1}{2}m\omega^2(r_1^2 + r_2^2) \tag{5.21}$$

$$H = H_{rel} + H_{cm} = \frac{1}{2\mu}p^2 + \frac{1}{2}\mu\omega^2 r^2 + \frac{1}{2M}P^2 + \frac{1}{2}M\omega^2 R^2 \tag{5.22}$$

If we could perform a full calculation, the wave function would factorize

$$|\Psi\rangle = |\psi_{rel}\rangle \otimes |\psi_{cm}\rangle \tag{5.23}$$

and since we are interested in the energy in the center-of-mass frame, $|\psi_{cm}\rangle$ should be the ground state. Any states in which $|\psi_{cm}\rangle$ is in an excited state are spurious. They are an artifact of the confining potential we have used to construct the basis. The lowest-lying spurious center-of-mass excitation will be a $1\hbar\omega$ excitation to a 1^- p-wave state. For a standard shell-model calculation performed in one oscillator shell, we cannot have any excitation of the center of mass. However, if we use two major shells, then there can be non-zero overlap between calculated states and the 1^- excitation of the center of mass.

The simplest remedy for this problem, proposed by Gloeckner and Lawson, is to add an additional term $\beta(H_{cm} - 3/2\hbar\omega)$, with β positive, to the Hamiltonian. This pushes excitations of the center of mass up in energy so that they no longer contaminate the low-energy spectrum. Technically, this is only valid if the relative and center-of-mass components of the wave function factorize, which is the case if all excitations up to a give $N\hbar\omega$ are included in the model space, as is done in the no-core shell model. However, this prescription is typically an effective cure for mild center-of-mass contamination.

5.5 Exercises

1. Show that, in the limit that no individual particle orbit is strongly occupied, the phonon creation operator of eq (5.14) has a bosonic commutation relation $\left[\mathcal{Q}^\dagger_\mu, \mathcal{Q}_{\mu'}\right] = \delta_{\mu\mu'}$. Hint: in the assumed limit, a_j acting on the one phonon state should give zero, as should $a^\dagger_b$.

Chapter 6

Methods for obtaining shell model interactions

In this section, I discuss some methods for obtaining the effective interactions to be used in shell model calculations.

6.1 Phenomenological methods

One approach (thus far the most successful) is to fit the interaction to data. One starts with an interaction obtained by one of the other methods mentioned below, and adjusts matrix elements, or some linear combination of matrix elements, in order to minimize the rms (root-mean-squared) deviation of the calculated levels from experiment. The gold standard of this approach is the USD interaction of Wildenthal and Brown, which can reproduce spectra in the *sd* shell to within ∼200 keV. In most cases, this global fit is not performed (or not feasible), and just a few matrix elements or monopoles are adjusted by hand, perhaps in an ad-hoc way, to better reproduce experiment.

6.2 Microscopic Approaches

I will now discuss the major microscopic approaches to obtaining an effective shell model Hamiltonian. The general idea is to devide the many-body Hilbert space into the model space, with projection operator P, and the excluded space, with projection operator Q. Some properties of these operators are:

$$P^2 = P, \quad Q^2 = Q, \quad PQ = QP = 0, \quad P + Q = \mathbb{I}. \tag{6.1}$$

The goal is to find some similarity transformation X such that the transformed Hamiltonian does not couple the P and Q spaces:

$$Q\tilde{H}P = 0 \quad \text{with} \quad \tilde{H} = X^{-1}HX. \tag{6.2}$$

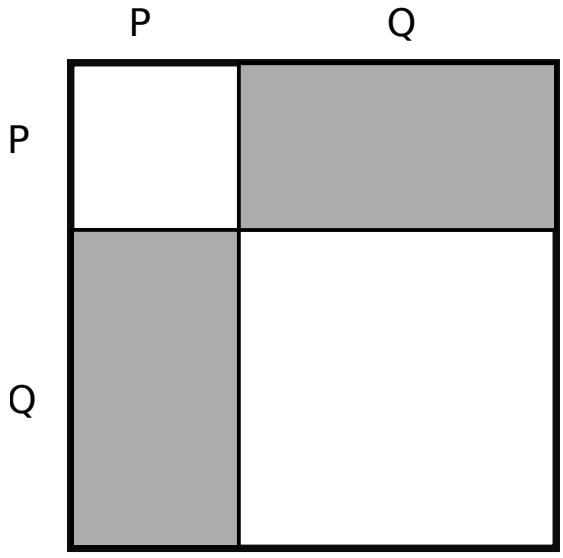

Figure 6.1: Schematic diagram of division of the Hilbert space in to P and Q spaces. The aim of microscopic approaches is to find some transformed Hamiltonian in which the two spaces are decoupled.

If such a transformation is found, then

$$\begin{aligned} H|\Psi_i\rangle &= E_i|\Psi_i\rangle \\ X^{-1}HXX^{-1}|\Psi_i\rangle &= E_iX^{-1}|\Psi_i\rangle \\ (P+Q)\tilde{H}(P+Q)\Big|\tilde{\Psi}_i\Big\rangle &= E_i\Big|\tilde{\Psi}_i\Big\rangle \\ (P\tilde{H}P+Q\tilde{H}Q)\Big|\tilde{\Psi}_i\Big\rangle &= E_i\Big|\tilde{\Psi}_i\Big\rangle \\ P\tilde{H}P\Big|\tilde{\Psi}_i\Big\rangle &= E_iP\Big|\tilde{\Psi}_i\Big\rangle \end{aligned} \tag{6.3}$$

and we see that the eigenvalues of the transformed operator in the P space exactly reproduce (some of) the eigenvalues of the full Hilbert space, which is exactly what we want in a shell model effective interaction. With a few additional lines of algebra, one may show that (see exercises)

$$XP\Big|\tilde{\Psi}_i\Big\rangle = |\Psi_i\rangle \tag{6.4}$$

that is, the P space component of the transformed wave function can be mapped back to the original full Hilbert-space wave function, by the transformation X. Our effective shell model interaction is then

$$H_{\text{eff}} \equiv P\tilde{H}P. \tag{6.5}$$

The remainder of this section outlines various methods for obtaining the similarity transformation X. It should be noted that in the case $X^{-1} = X^\dagger$, then X

is a *unitary transformation*. This is particularly important for obtaining matrix elements of operators other than the Hamiltonian.

6.2.1 Many-body perturbation theory

Since there is no way to cover MBPT in a fraction of a lecture, I'll focus here on what is called Rayleigh-Schrödinger (RS) perturbation theory. In RS perturbation theory, the similarity transformation is typically called a *wave operator*, and denoted Ω, but for consistency I'll stick with X. We write the wave operator as

$$X = 1 + \chi \quad \text{with} \quad \chi = Q\chi P. \tag{6.6}$$

The operator χ is called the correlation operator, and it accounts for effects outside of the model space. Note that $\chi^2 = 0$ and so $X^{-1} = 1 - \chi$. The effective Hamiltonian is

$$H_{\text{eff}} = PHP + PH\chi. \tag{6.7}$$

We could expand χ in terms of powers of the interaction. However, this leads to divergences due to degenerate orbits in the model space. Instead, we'll discuss an iterative approach (called folded diagrams). Our requirement that $Q\tilde{H}P = 0$ becomes

$$\begin{aligned} 0 &= Q(1-\chi)H(1+\chi)P \\ &= QHP - \chi PHP + QH\chi - \chi H\chi \end{aligned} \tag{6.8}$$

We may then rearrange this to solve for χ, (adding $PHP\chi = 0$ to the lhs)

$$\begin{aligned} (PHP - QHQ)\chi &= QHP - \chi PHP - \chi PHQ\chi \\ (PHP - QHQ)\chi &= QHP - \chi H_{\text{eff}} \\ \chi &= \frac{1}{PHP - QHQ}(QHP - \chi H_{\text{eff}}). \end{aligned} \tag{6.9}$$

The idea is then to solve this and obtain H_{eff}. One way to do this is to multiply both sides of (6.9) by PH and add PHP, which gives

$$\begin{aligned} PHP + PH\chi &= PHP + PH\frac{1}{PHP - QHQ}QHP - PH\frac{1}{PHP - QHQ}\chi H_{\text{eff}} \\ H_{\text{eff}} &= \hat{Q}_{\text{box}} - PH\frac{1}{PHP - QHQ}\chi H_{\text{eff}} \end{aligned} \tag{6.10}$$

where I have defined the Q-box operator

$$\hat{Q}_{\text{box}} \equiv PHP + PH\frac{1}{PHP - QHQ}QHP. \tag{6.11}$$

Typically, PHP is replaced by a *starting energy* ω, and the Q-box is written $\hat{Q}_{\text{box}}(\omega)$. If we insert (6.9) into (6.10), we obtain

$$\begin{aligned} H_{\text{eff}} &= \hat{Q}_{\text{box}} + \sum_{m=1}^{\infty} \frac{(-1)^m}{(\omega - QHQ)^{m+1}} QHPH_{\text{eff}}^m \\ &= \hat{Q}_{\text{box}} + \sum_{m=1}^{\infty} \frac{1}{m!} \frac{\partial^m \hat{Q}_{\text{box}}}{\partial \omega^m} H_{\text{eff}}^m. \end{aligned} \tag{6.12}$$

Typically, the expression for $\hat{Q}_{\rm box}(\omega)$ is calculated in perturbation theory up to second or third order using ($H = H_0 + H_1$)

$$\frac{1}{\omega - QHQ} = \frac{1}{\omega - QH_0Q} + \frac{1}{\omega - QH_0Q} H_1 \frac{1}{\omega - QH_0Q} + \frac{1}{\omega - QH_0Q} H_1 \frac{1}{\omega - QH_0Q} H_1 \frac{1}{\omega - QH_0Q} + \ldots \tag{6.13}$$

and (6.12) is iterated until convergence.

6.2.2 The Lee-Suzuki method

Another approach is typically called the Lee-Suzuki method. We take the equation for the effective operator

$$PH_{\rm eff}P = PHP + PHQ\chi P \tag{6.14}$$

which solves the Schrödinger equation for some subset of the eigenstates $|k\rangle$ of the full Hamiltonian:

$$PH_{\rm eff}|k_{\rm eff}\rangle = E_k|k_{\rm eff}\rangle. \tag{6.15}$$

Here, the effective wave function is given by

$$|k_{\rm eff}\rangle = X^{-1}|k\rangle = (1-\chi)|k\rangle. \tag{6.16}$$

Plugging this in, we have

$$\begin{aligned}
(PHP + PHQ\chi P)(1+\chi)|k\rangle &= E_k(1-\chi)|k\rangle \\
(PHP + PHQ\chi P)|k\rangle &= PE_k|k\rangle \\
(PHP + PHQ\chi P)|k\rangle &= (PHP + PHQ)|k\rangle \\
PHQ\chi P|k\rangle &= PHQ|k\rangle \\
Q\chi P|k\rangle &= Q|k\rangle.
\end{aligned} \tag{6.17}$$

This may be written as

$$\begin{aligned}
\sum_{\alpha_P} \langle\alpha_Q|\chi|\alpha_P\rangle\langle\alpha_P|k\rangle &= \langle\alpha_Q|k\rangle \\
\sum_{\alpha_P k} \langle\alpha_Q|\chi|\alpha_P\rangle\langle\alpha_P|k\rangle\langle\tilde{k}|\alpha'_P\rangle &= \sum_k \langle\alpha_Q|k\rangle\langle\tilde{k}|\alpha'_P\rangle \\
\langle\alpha_Q|\chi|\alpha'_P\rangle &= \sum_k \langle\alpha_Q|k\rangle\langle\tilde{k}|\alpha'_P\rangle.
\end{aligned} \tag{6.18}$$

In these equations $\langle\tilde{k}|\alpha_P\rangle$ is the inverse of $\langle\alpha|k\rangle$, i.e. $\sum_k \langle\alpha_P|k\rangle\langle\tilde{k}|\alpha'_P\rangle = \delta_{PP'}$. We therefore have an equation for all the matrix elements of χ. Note that this requires us to know the eigenstates in the large space before we can produce the effective Hamiltonian for the small space. So, for example, in order to produce an sd shell effective interaction, we would need to solve a 16-body problem to get the core energy, a 17-body problem to get the single particle energies, and an 18-body problem to get the two-body matrix elements. This has been achieved both with the no-core shell model, and with coupled cluster theory.

6.2.3 In-medium SRG

As in the previous methods, we wish to obtain a unitarily-transformed Hamiltonian $\tilde{H}$ such that $Q\tilde{H}P = 0$. We define the transformation in terms of an anti-hermitian operator Ω:

$$\tilde{H} = e^{\Omega} H e^{-\Omega} \quad , \quad \Omega^{\dagger} = -\Omega. \tag{6.19}$$

Here, we do not make the simplifying Lee-Suzuki assumption that $Q\Omega Q = P\Omega P = 0$. Instead, we write the transformed Hamiltonian as an infinite series of commutators

$$e^{\Omega} H e^{-\Omega} = H + [\Omega, H] + \frac{1}{2!}[\Omega, [\Omega, H]] + \dots \tag{6.20}$$

and press on with the faith that some finite number of commutators will be sufficient. The impatient reader will note that we still have yet to solve for Ω. In fact, we will not obtain Ω analytically. Instead, we will make a guess and refine this guess until we are satisfied.

We call the initial guess η, which we choose based on the Hamiltonian H. We then transform H according to η to obtain a new Hamiltonian, and choose a new η based on that Hamiltonian. The manner in which we choose η is arbitrary so long as it helps reduce the off-diagonal component of H – though some choices work better than others. After n iterations, we have our transformed Hamiltonian

$$\tilde{H}_n = e^{\eta_n} \dots e^{\eta_1} H e^{-\eta_1} \dots e^{-\eta_n}. \tag{6.21}$$

For concreteness, I now illustrate a specific choice of generator, due to White. If we consider a 2×2 Hamiltonian, the corresponding anti-hermitian generator has just one parameter, θ

$$H_{2\times 2} = \begin{pmatrix} \epsilon_1 & h_{od} \\ h_{od} & \epsilon_2 \end{pmatrix} \quad , \quad \Omega_{2\times 2} = \begin{pmatrix} 0 & \theta \\ -\theta & 0 \end{pmatrix}. \tag{6.22}$$

The unitary transformation e^{Ω} is simply a rotation matrix in the plane

$$e^{\Omega_{2\times 2}} = \begin{pmatrix} \cos\theta & \sin\theta \\ -\sin\theta & \cos\theta \end{pmatrix} \tag{6.23}$$

and the angle which diagonalizes $H_{2\times 2}$ is given by

$$\tan 2\theta = \frac{2h_{od}}{\epsilon_1 - \epsilon_2}. \tag{6.24}$$

For the 2×2 case, this is an exact solution, and expanding the transformation in an infinite series of commutators is overkill. But if we expand to just a 3×3 case, a closed-analytic solution is a nightmare. So we guess that the solution looks similar to the 2×2 case, and iterate.

Returning to our many-body case, we have the choice for η:

$$\langle i|\eta|j\rangle = \frac{1}{2}\tan^{-1}\left(\frac{2\langle i|H|j\rangle}{\langle i|H|i\rangle - \langle j|H|j\rangle}\right). \tag{6.25}$$

There is a further complication in the many-body problem, in that Ω and η may contain up to A-body operators, which is essentially impossible to deal with. Even if we start with a two-body interaction, the infinite series of commutators will induce higher-body terms. We cannot eliminate this, but we can minimize it and ignore it.

6.3 Methods for treating bare interactions

6.3.1 Brueckner G matrix

Up until the past decade or so, essentially all NN interactions V_{NN} had a strong repulstive core, and so performing a perturbation expansion in terms of powers of V_{NN} was hopeless. The Brueckner G-matrix is a technique for circumventing this issue by non-perturbatively calculating certain classes of diagrams (so called *ladder diagrams*) to infinite order. The perturbative expansion for the ground state energy is

$$E_0 = \frac{1}{2}\sum_{ab}\langle ab|V|ab\rangle + \frac{1}{2^2}\sum_{abij}\frac{\langle ab|V|ij\rangle\langle ij|V|ab\rangle}{\epsilon_a+\epsilon_b-\epsilon_i-\epsilon_j} + \frac{1}{2^3}\sum_{abijkl}\frac{\langle ab|V|ij\rangle\langle ij|V|kl\rangle\langle kl|V|ab\rangle}{(\epsilon_a+\epsilon_b-\epsilon_i-\epsilon_j)(\epsilon_a+\epsilon_b-\epsilon_k-\epsilon_l)} + \dots \tag{6.26}$$

The general idea can be explained as this: if we consider the function $f(x) = \frac{x}{1+x}$, we may Taylor exand it in powers of x:

$$\frac{x}{1+x} = x - x^2 + x^3 - x^4 + \dots \tag{6.27}$$

This expansion converges for $x < 1$. However, the function $f(x)$ is still finite for all $x \neq -1$.

With this in mind, we assume that the result is finite and write

$$E_0 \equiv \frac{1}{2}\langle ab|G|ab\rangle \tag{6.28}$$

where evidently

$$\begin{aligned}\frac{1}{2}\langle ab|G|ab\rangle &= \frac{1}{2}\langle ab|V|ab\rangle + \frac{1}{2}\sum_{ij}\frac{\langle ab|V|ij\rangle}{\epsilon_a+\epsilon_b-\epsilon_i-\epsilon_j}\left(\frac{1}{2}\langle ij|V|ab\rangle + \frac{1}{4}\sum_{kl}\frac{\langle ij|V|kl\rangle\langle kl|V|ab\rangle}{\epsilon_a+\epsilon_b-\epsilon_k-\epsilon_l} + \dots\right) \\ &= \frac{1}{2}\langle ab|V|ab\rangle + \frac{1}{2}\sum_{ij}\frac{\langle ab|V|ij\rangle}{\epsilon_a+\epsilon_b-\epsilon_i-\epsilon_j}\left(\frac{1}{2}\langle ij|G|ab\rangle\right)\end{aligned} \tag{6.29}$$

and we are left with an integral equation for G

$$G_{abab} = V_{abab} + \frac{1}{2}\sum_{ij}\frac{V_{abij}}{\epsilon_a+\epsilon_b-\epsilon_i-\epsilon_j}G_{ijab}. \tag{6.30}$$

6.3.2 Free-space Similarity Renormalization Group

In the free space SRG, we want to suppress terms in the Hamiltonian that couple low-momentum states to high-momentum states. This is achieved by using the kinetic energy as the generator, which drives the Hamiltonian to a diagonal form in momentum space.

6.3.3 $V_{\mathbf{low}k}$

In the V_{lowk} formulation for producing a low-momentum interaction, the Lee-Suzuki method is applied, with the difference being that the P and Q operators are defined in momentum space, and the low momentum part is decoupled from the high-momentum part.

6.4 Exercises

1. Prove equation (6.4). Hint: since $\tilde{H}$ decouples the P and Q spaces, we may replace PHP with $(P+Q)HP = HP$ in equation (6.3).

2. Derive the expansion for $\hat{Q}_{\text{box}}$ given in (6.13). Keep in mind that $\frac{1}{\omega - QHQ}$ is short hand for the inverse operator $(\omega - QHQ)^{-1}$.

Bibliography

[1] C. A. Bertulani. *Nuclear Physics in a Nutshell*. Princeton University Press, Princeton, 2007.

[2] J. M. Blatt and V. F. Weisskopf. *Theoretical Nuclear Physics*. Springer-Verlag, New York, 1979.

[3] D. Bohm. *Quantum Theory*. Prentice-Hall, New York, 1951.

[4] A. Bohr and B. R. Mottleson. *Nuclear Structure*. W. A. Benjamin, Inc., New York, 1 edition, 1969.

[5] B. A. Brown. *Lecture Notes in Nuclear Structure Physics*. 2010.

[6] G. E. Brown. *Unified Theory of Nuclear Models*. North Holland Publishing Co., Amsterdam, 1964.

[7] E. Caurier, G. Martínez-Pinedo, F. Nowacki, A. Poves, and A. P. Zuker. The shell model as a unified view of nuclear structure. *Rev. Mod. Phys.*, 77(April):427–488, 2005.

[8] A. De-Shalit and I. Talmi. *Nuclear Shell Theory*. Academic Press, 1963.

[9] A. L. Fetter and J. D. Walecka. *QuantumTheory of Many-Particle Systems*. Dover Publications, Inc, Mineola, 2003.

[10] D. H. Gloeckner and R. D. Lawson. Spurious center-of-mass motion. *Phys. Lett. B*, 53(4):313–318, 1974.

[11] M. G. Mayer. Nuclear configurations in the spin-orbit coupling model. I. Empirical evidence. *Phys. Rev.*, 78(1):16, 1950.

[12] M. G. Mayer. Nuclear Configurations in the Spin-Orbit Coupling Model. II. Theoretical Considerations. *Phys. Rev.*, 78(1):22, 1950.

[13] T. Otsuka, T. Suzuki, R. Fujimoto, H. Grawe, and Y. Akaishi. Evolution of Nuclear Shells due to the Tensor Force. *Phys. Rev. Lett.*, 95(23):232502, November 2005.

[14] O. Sorlin and M.-G. Porquet. Nuclear magic numbers: New features far from stability. *Prog. Part. Nucl. Phys.*, 61(2):602–673, October 2008.

[15] J. Suhonen. *From Nucleons to Nucleus.* Springer, 2007.